HELDA
HELSINGIN YLIOPISTO
HELSINGFORS UNIVERSITET
UNIVERSITY OF HELSINKI

UNIVERSITY OF HELSINKI

https://helda.helsinki.fi

Acid-Base Clusters during Atmospheric New Particle Formation in Urban Beijing

Yin, Rujing

2021-08-17

Yin , R , Yan , C , Cai , R , Li , X , Shen , J , Lu , Y , Schobesberger , S , Fu , Y , Deng , C , Wang , L , Liu , Y , Zheng , J , Xie , H , Bianchi , F , Worsnop , D R , Kulmala , M & Jiang , J 2021 , ' Acid-Base Clusters during Atmospheric New Particle Formation in Urban Beijing ' , Environmental Science & Technology , vol. 55 , no. 16 , pp. 10994-11005 . https://doi.org/10.1021/acs.est.1c02701

http://hdl.handle.net/10138/347041
https://doi.org/10.1021/acs.est.1c02701

unspecified
acceptedVersion

Downloaded from Helda, University of Helsinki institutional repository.

This is an electronic reprint of the original article.

This reprint may differ from the original in pagination and typographic detail.

Please cite the original version.

Acid-base clusters during atmospheric new particle formation in urban Beijing

Rujing Yin[1], Chao Yan[2,3], Runlong Cai[3], Xiaoxiao Li[1], Jiewen Shen[4], Yiqun Lu[5], Siegfried Schobesberger[6], Yueyun Fu[1], Chenjuan Deng[1], Lin Wang[5], Yongchun Liu[2], Jun Zheng[7], Hongbin Xie[4], Federico Bianchi[2,3], Douglas R. Worsnop[3,8], Markku Kulmala[2,3], Jingkun Jiang[1]*

[1] State Key Joint Laboratory of Environment Simulation and Pollution Control, School of Environment, Tsinghua University, Beijing 100084, China.

[2] Aerosol and Haze Laboratory, Beijing Advanced Innovation Center for Soft Matter Science and Engineering, Beijing University of Chemical Technology, Beijing 100084, China.

[3] Institute for Atmospheric and Earth System Research / Physics, Faculty of Science, University of Helsinki, 00014 Helsinki, Finland.

[4] Key Laboratory of Industrial Ecology and Environmental Engineering (Ministry of Education), School of Environmental Science and Technology, Dalian University of Technology, Dalian 116024, China

[5] Shanghai Key Laboratory of Atmospheric Particle Pollution and Prevention (LAP3), Department of Environmental Science and Engineering, Fudan University, Shanghai 200433, China

[6] Department of Applied Physics, University of Eastern Finland, Kuopio, Finland

[7] Jiangsu Key Laboratory of Atmospheric Environment Monitoring and Pollution Control, Nanjing University of Information Science & Technology, Nanjing 210044, China

[8] Aerodyne Research Inc., Billerica, Massachusetts 01821, USA

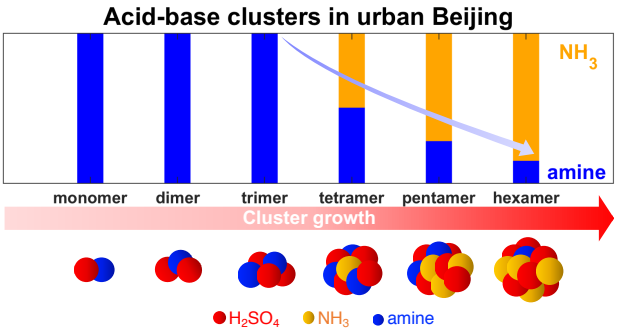

26

27 TOC Art

28

ABSTRACT. Molecular clustering is the initial step of atmospheric new particle formation (NPF) that generates numerous secondary particles. Using two online mass spectrometers with and without a chemical ionization inlet, we characterized the neutral clusters and the naturally charged ion clusters during NPF periods in urban Beijing. In ion clusters, we observed pure sulfuric acid (SA) clusters, SA-amine clusters, SA-ammonia (NH_3) clusters, and SA-amine-NH_3 clusters. However, only SA clusters and SA-amine clusters were observed in neutral form. Meanwhile, oxygenated organic molecule (OOM) clusters charged by a nitrate ion and a bisulfate ion were observed in ion clusters. Acid-base clusters correlate well with the occurrence of sub-3 nm particles, whereas OOM clusters do not. Moreover, with the increasing cluster size, amine fractions in ion acid-base clusters decrease while NH_3 fractions increase. This variation results from the reduced stability differences between SA-amine clusters and SA-NH_3 clusters, which is supported by both quantum chemistry calculations and chamber experiments. The lower average number of dimethylamine (DMA) molecules in atmospheric ion clusters than the saturated value from controlled SA-DMA nucleation experiments suggests there is insufficient DMA in urban Beijing to fully stabilize large SA clusters and therefore, other basic molecules like NH_3 play an important role.

KEYWORDS: Urban Beijing, Ion clusters, Neutral clusters, Acid-base clustering, Average base number

SYNOPSIS: Composition of ion and neutral clusters reveals key clustering steps and precursors contributing to atmospheric new particle formation in urban Beijing.

1 Introduction

New particle formation (NPF) is a significant source of atmospheric particles[1]. Multistep clustering is the initial process of NPF and direct observation of the molecular cluster composition can help to reveal the clustering pathways and the key gaseous precursors for NPF[2, 3]. Both neutral clusters and naturally charged clusters, referred to as ion clusters hereafter, exist in the atmosphere[4], and simultaneous measurements of both are often required for understanding NPF mechanism. Neutral clusters can be selectively measured using chemical ionization mass spectrometry[5, 6]. During the chemical ionization process, however, base molecules may dissociate from clusters such that the original cluster information is lost[7, 8]. Ion clusters can be measured directly using mass spectrometers without the chemical ionization unit[9], and thus, more complete information might be preserved when measuring ion clusters[10]. For instance, SA-ammonia (NH_3) clusters were mostly detected as ion clusters but not as neutral ones in chamber experiments[11]. While for SA-dimethylamine (DMA) clusters, whose stabilities are higher than SA-NH_3 clusters when the number of SA and base molecules are the same[12-14], both neutral and ion ones were detected[15, 16].

There have been only a few simultaneous measurements of atmospheric ion clusters and neutral clusters, which are in rural and remote areas such as Hyytiälä, Jungfraujoch, and Aboa[17-19]. At these sites, ion acid-base clusters consisting of up to 10 SA molecules and several NH_3 molecules were observed[17-19]. Meanwhile, base molecules were not observed in neutral SA clusters[17-19], which may be due to the dissociation of NH_3 or other base molecules upon the chemical ionization. Moreover, ion clusters of oxygenated organic molecules (OOMs) were also observed occasionally in Hyytiälä and Jungfraujoch. Based on these measurements, it was proposed that SA-NH_3 and organics contribute primarily to the clustering pathways in these environments[17-19].

In urban atmospheric environments, the complex mixture of gas precursors and potential clustering molecules may lead to different clustering pathways. Measurement of neutral clusters in urban Shanghai[20] was reported without the information of ion

clusters. In the meantime, neutral SA-DMA clusters containing 3-4 SA molecules and 1-2 DMA molecules were observed[20]. Similar to those in clean environments, neutral SA-NH_3 clusters were not observed in Shanghai, probably resulted from both their chemical ionization fragmentation and low concentrations. Nevertheless, the importance of DMA in the initial step of clustering in urban areas was attested.

The relative stability of SA-DMA clusters in comparison to SA-NH_3 clusters varies as a function of the cluster size. According to the quantum chemical calculation, the number of hydrogen bonds and the proton affinity of bases mainly affect the stability of acid-base clusters[21]. As DMA has higher proton affinity than NH_3, for both ion and neutral acid-base clusters, the formation of SA-DMA clusters containing four SA molecules or less has lower formation free energies than that of SA-NH_3 clusters with the same number of SA molecules[13]. Thus, in these small sizes, SA-DMA clusters are more stable than SA-NH_3 clusters. For larger clusters, their structure and stabilities are less established owing to the large uncertainty of the simulation by quantum chemical calculations. However, it is predicted that NH_3-containing clusters would gain an advantage in larger sizes as NH_3 can form more hydrogen bonds than DMA[22, 23]. Flow tube experiments showed that the substitution of NH_3 by DMA in clusters becomes slower with the increase in the clusters size[24]. Moreover, controlled chamber experiments showed that the uptake of NH_3 in 10-30 nm nanoparticles is more preferred than that of DMA since the particulate ammonium-to-dimethylaminium ratios were higher than the gaseous NH_3-to-DMA ratios[25]. In the meanwhile, kinetics also affects the clustering. For example, when the concentration of NH_3 is several orders of magnitude higher than that of DMA, NH_3 collides more frequently with clusters than DMA, which makes up the difference in stability. Therefore, NH_3 can enhance the cluster formation rate by forming SA-DMA-NH_3 clusters[21, 26, 27].

In addition to SA, DMA and NH_3, other amines and organics may also contribute to the clustering in urban atmospheric environments. Methylamine (MA, C_1-amine) and trimethylamine (TMA, C_3-amine) have been shown to efficiently cluster with SA molecules by both quantum chemical calculation and controlled flow tube

experiments[28, 29]. Similar to DMA, their concentrations in urban environments are often higher than those in rural areas[30, 31]. In addition, there is a high abundance of other anthropogenic organic compounds in urban environments from anthropogenic emissions[32], which could also facilitate the clustering. Oxidized biogenic organic compounds (BioOxOrg) were shown to cluster by themselves or with SA and NH_3 in Cosmics Leaving OUtdoor Droplets (CLOUD) chamber experiments, and clusters containing several BioOxOrg molecules were observed both as neutral clusters and ion clusters[3, 33-35]. The involvement of these species in the clustering, especially during NPF periods, is still uncertain in urban areas.

In this study, we characterized both atmospheric neutral clusters and ion clusters during two seasons in urban Beijing. Gaseous precursors and particle size distributions down to ~ 1 nm were also monitored. The composition of both neutral clusters and ion clusters during NPF periods was revealed. Their correlations with the newly formed sub-3 nm particles were examined. We also examined the dependence of cluster composition on the cluster size and the contributions of different gas precursors. These findings were compared to those from CLOUD chamber experiments and clean atmospheric environments.

2 Methods

2.1 Field Measurement

The sampling site is located at the west campus of Beijing University of Chemical Technology (39°94'N, 116°30'E), near the 3rd-Ring road of Beijing. It is on the top floor of an office building, ~20 m above the ground. Details of the site can be found in our previous studies[36-38]. The measurement campaign was from Feb. 14th to 27th, 2108 (period 1) and from Nov. 9th to 28th, 2018 (period 2).

Ion clusters were measured using an atmospheric pressure interface high-resolution time-of-flight mass spectrometer (APi-HTOF or APi-LTOF, Aerodyne Research, Inc.)[9]. APi-HTOF with the mass resolution of ~4500 (at 200 Th) was used during period 1 and APi-LTOF with the mass resolution of ~8000 (at 200 Th) was used during period 2.

Ambient air was sampled from the window through a 1.4 m long 1/4-inch stainless steel tubing. The sample flow rate was 0.8 lpm with a bypass flow of 3.0 lpm. The mass spectrometer was running in the negative ion mode to measure the negatively charged ion clusters. The 1-s resolution data was averaged to hourly resolution to ensure a good signal-to-noise ratio so that the cluster composition can be reliably identified. Since the absolute concentration of ion clusters was not calibrated, the integrated signal intensities were used.

Neutral clusters were measured using a chemical ionization atmospheric pressure interface high-resolution time-of-flight mass spectrometer (CI-APi-HTOF or CI-APi-LTOF, Aerodyne Research, Inc.) equipped with a nitrate inlet[5]. Gaseous SA and oxygenated organic molecules (OOMs) were measured simultaneously. CI-APi-LTOF with the mass resolution of ~8000 was used during period 1 and CI-APi-HTOF with the mass resolution of ~4000 was used during period 2. Ambient air was sampled through a 1.4 m long 3/4 inch stainless steel tubing. The sample flow rate was 0.8 lpm with a bypass flow of 8 lpm. Details of the flowrate settings and data processing were similar to Lu et al[39]. Nitrate ion (NO_3^-) and its clusters ($(HNO_3)_{1-2}NO_3^-$) were used as the reagent ions to ionize neutral clusters and gaseous species, e.g. SA and OOMs. Nitric acid vapors were volatilized from a glass tube and carried by zero air of 20 lpm into the inlet, then they were exposed to soft X-ray to produce NO_3^- and its clusters ($(HNO_3)_{0-2}NO_3^-$). The time of the ion-molecule reactions within the CI-inlet was ~200 ms. The CI-APi-HTOF (or CI-APi-LTOF) was running in the negative ion mode with a time resolution of 1 s and was averaged to 5 min. Calibrations of sulfuric acid sensitivity and mass-dependent transmission efficiency were performed following Kürten et al.[40] and Heinritzi et al.[41], respectively. The calibration factors for SA of CI-APi-LTOF (period 1) and CI-APi-HTOF (period 2) are 1.1×10^{10} and 7.74×10^{8} cm^{-3}, respectively, and the relative transmission efficiency curves of APi-TOF and CI-APi-TOF are shown in Figure S1 in the supplementary information (SI).

Particle size distributions were measured using a diethylene glycol scanning mobility particle sizer (DEG-SMPS)[42, 43] and a particle size distribution system (PSD)[44]. The

DEG-SMPS and the PSD measure particles in the size ranges of 1-6.5 nm and 3 nm–10 μm, respectively, both with a time resolution of 5 min. The DEG-SMPS was equipped with a specially designed differential mobility analyzer[43] and a core sampling apparatus[45] for nanoparticles. The condensation sink (CS), which represents the coagulation scavenging of particles was calculated based on the measured particle size distributions according to Eq. S1 in the SI.

2.2 Data Analysis

The average base number (ABN_n) was calculated and used as an index to characterize the acid to base ratio in acid-base clusters such as SA-NH_3 clusters, SA-amine clusters, and SA-amine-NH_3 clusters. The subscript "*n*" indicates the number of SA molecules (including the bisulfate ion) in an SA-base cluster. ABN_n is defined as the average number of base molecules in SA-base clusters containing the same number of SA molecules. Schobesberger et al.[46] have calculated the ABN of SA-NH_3 ion clusters detected in controlled CLOUD controlled experiments. In this study, the average number of both amines and NH_3 ($m_{amine,n}$ and $m_{NH3,n}$) are included when evaluating ABN_n. The calculation is shown below:

$$\mathrm{ABN}_n = \frac{\sum\left(m_{1,n} \times s_{n,m_1,m_2}\right) + \sum\left(m_{2,n} \times s_{n,m_1,m_2}\right)}{\sum s_{n,m_1,m_2}} \quad (1)$$

$$m_{amines,n} = \frac{\sum\left(m_{1,n} \times s_{n,m_1,m_2}\right)}{\sum s_{n,m_1,m_2}} \quad (2)$$

$$m_{NH_3,n} = \frac{\sum\left(m_{2,n} \times s_{n,m_1,m_2}\right)}{\sum s_{n,m_1,m_2}} \quad (3)$$

$$\mathrm{ABN}_n = m_{amines,n} + m_{NH_3,n} \quad (4)$$

where $m_{1,n}$ is the number of amine molecules in an acid-base cluster with *n* sulfuric acid molecules; $m_{2,n}$ is the number of NH_3 molecules in an acid-base cluster with *n* sulfuric acid molecules; $s_{n,m1,m2}$ is the signal intensity of an acid-base cluster containing *n* SA molecules (including HSO_4^-), m_1 amine molecules, and m_2 NH_3 molecules. In this study,

186 ABN_n was only calculated for naturally charged ion acid-base clusters because NH_3-
187 containing clusters were not observed in neutral clusters.

188 **3 Results & Discussion**

189 **3.1 Typical Composition of Ion Clusters and Neutral Clusters**

190 During NPF periods in urban Beijing, we observed ion acid-base clusters containing
191 SA, NH_3, and amine molecules (Fig. 1). The identified ion acid-base clusters were
192 categorized into five types, including SA clusters ($(H_2SO_4)_{0\text{-}3}HSO_4^-$), SA-amine
193 clusters ($(H_2SO_4)_{2\text{-}3}(amine)_{1\text{-}2}HSO_4^-$), SA-$NH_3$ clusters ($(H_2SO_4)_{3\text{-}5}(NH_3)_{1\text{-}4}HSO_4^-$),
194 SA-amine-NH_3 clusters ($(H_2SO_4)_{4\text{-}5}(amine)_{1\text{-}2}(NH_3)_{1\text{-}3}HSO_4^-$), and SA-amine (-$NH_3$)
195 clusters, which are hydrogen bonded[21, 47]. Here, SA-amine (-NH_3) clusters could be
196 either SA-amine clusters or SA-amine-NH_3 clusters due to possible isomers, and
197 amines include C_n-amines (n=1, 2, 3, 4, corresponding to CH_5N, C_2H_7N, C_3H_9N, and
198 $C_4H_{11}N$, respectively). Based on the number of SA molecules in these clusters (Table
199 S1), they can be referred to as monomer (A_1), dimer (A_2), trimers ($A_3B_{0\text{-}1}$), tetramers
200 ($A_4B_{0\text{-}2}$), pentamers ($A_5B_{1\text{-}3}$), and hexamers ($A_6B_{2\text{-}4}$). Here, A represents sulfuric acid
201 and B represents bases (i.e., NH_3 or amines). With the increase in the cluster size,
202 amines and NH_3 appeared sequentially in these acid-base clusters. $C_{2,3,4}$-amines
203 appeared from trimers while C_1-amine and NH_3 appeared from tetramers onwards. SA-
204 amine-NH_3 clusters appeared from pentamers onwards. Similar appearance patterns
205 were observed in controlled chamber experiments[11, 16, 48]. In addition to acid-base
206 clusters, ion clusters of OOMs charged by nitrate ion and bisulfate ion, i.e., OOM-NO_3^-
207 and OOM-HSO_4^- clusters, were also observed in urban Beijing (Fig. 1). The observed
208 OOMs include non-nitrate OOMs and organonitrates. Similar composition of ion OOM
209 clusters has been observed in Hyytiälä[49], and we will compare them in detail later.

210 ==========

211 Place Figure 1 Here

212 ==========

During the same NPF periods, neutral acid-base clusters containing SA and amine molecules were also observed (Fig. 1). They were detected in the form of SA clusters ($(H_2SO_4)_{0-2}HSO_4^-$) and SA-amine clusters ($(H_2SO_4)_2(amine)HSO_4^-$), including monomer, dimer, and trimers. In these neutral clusters, $C_{1,2,3,4}$-amines all appeared in trimers and NH_3 was not observed. Neutral OOM clusters charged by nitrate ion were also observed (Fig. 1). However, different from ion OOM clusters, which are formed naturally in the atmosphere, the counts of neutral OOM-NO_3^- clusters reflect the mixing ratios of gaseous OOMs as the clusters are formed through the reaction between gaseous OOMs and the reagent ion, NO_3^-, in the chemical ionization unit[50]. OOM-HSO_4^- clusters were not identified in the measured neutral clusters. Note that during a previous study in urban Shanghai[20], neutral SA-DMA trimers were observed as well (Fig. S2).

During our measurements in urban Beijing, the appearance of acid-base clusters was coincident with the occurrence of sub-3 nm particles, while OOM clusters did not show a significant correlation with sub-3 nm particles. It was reflected on several aspects. Firstly, comparing the cluster composition observed during NPF periods and non-NPF periods, the existence of large ion acid-base clusters (i.e., clusters containing 4-6 SA molecules) is the main difference, while the composition of ion OOM clusters and neutral OOM clusters did not change much (comparing Figs. 1 and S3). Secondly, the concentrations of neutral acid-base clusters and signals of ion acid-base clusters synchronized well with the number concentration of sub-3 nm particles (Fig. 2). They all peaked during the NPF periods, closely followed by the formation of gaseous sulfuric acid, a key NPF precursor. During the days when CS was low (i.e., < 0.02 s^{-1})[36, 51], which facilitated the occurring of NPF events, the acid-base clusters emerged largely together with sub-3 nm particles. Thirdly, these ion and neutral acid-base clusters have good correlations with sub-3 nm particles (r^2=0.31~0.8), disregarding the neutral monomer and ion monomer (Fig. S4). This good correlation between clusters and newly formed particles has also been observed in other atmospheric measurements[17-19] and chamber experiments[11, 16], where these clusters were usually

representative for the clustering pathway during NPF. Fourthly, there are no significant correlations between ion OOM clusters and sub-3 nm particles, and the median r^2 was 0.04 for OOM-HSO_4^- and 0.008 for OOM-NO_3^- clusters (Fig. S5). The above observations were confirmed during another season in Beijing. As shown in Fig. S6, the composition of neutral clusters and ion clusters during NPF periods in Nov. 2018 is similar. The good correlations between acid-base clusters and sub-3 nm particles were observed in Nov. 2018 as well (Fig. S7).

==========

Place Figure 2 Here

==========

In Beijing, the measured ion acid-base clusters and neutral acid-base clusters showed different characteristics in size range and composition. Firstly, ion acid-base clusters were measured from monomer to hexamers, while only monomer, dimer, and trimers were seen in neutral modes. This could be related with the low concentrations of large neutral clusters in the atmosphere or their fragmentation in mass spectrometers and chemical ionization. In mass spectrometers, weakly bonded clusters such as ion NH_3-containing clusters would experience collision-induced dissociation to some extent while stable ones such as ion SA-DMA clusters would not[52]. Chemical ionization of neutral clusters also causes the evaporation of base molecules or base-containing clusters, leading to the complete evaporation of NH_3 molecules in monomer, dimer, and trimers[8]. DMA would completely evaporate from the ionized monomer and dimers, thus for DMA and NH_3, the smallest base-containing clusters that can be detected are trimers and tetramers, respectively[8]. Due to the lack of binding energy of SA-DMA-NH_3 clusters, the influence of ionization on such clusters is unclear, but NH_3 was reported to evaporate more easily than DMA in neutral SA-DMA-NH_3 clusters[53]. Secondly, NH_3-containing clusters were observed only in ion clusters from tetramers to hexamers. Ion clusters grow by adding SA molecules from monomer to trimers. This is because the charge (i.e. HSO_4^-), which can stabilize clusters as a Lewis base, prevents

the addition of NH_3 until tetramers[54], which is consistent with chamber experiments[55]. However, it cannot be determined whether NH_3 is contained in neutral clusters from the measured results, because NH_3-containing clusters are likely to evaporate during chemical ionization or in the low-pressure region inside mass spectrometers.

Ion acid-base clusters observed during NPF periods in urban Beijing have more complicated composition and smaller size range when comparing to those observed in clean areas such as Hyytiälä[17], Jungfraujoch[18], and Aboa[19] (Fig. 3), due to their different atmospheric environments, including the abundance of amines, the scavenging rate of ion clusters, and the formation pathway of OOMs. Firstly, while both SA clusters and SA-NH_3 clusters were observed in these four sites, amine-containing ion clusters (i.e., SA-amine clusters and SA-amine-NH_3 clusters) were only observed in urban Beijing, indicating the relatively high abundance of amines in urban atmospheres. Secondly, ion clusters containing 7-10 SA molecules were observed in the other three sites except for urban Beijing, due to the high CS in the latter place. The total ion production rates were reported to be in the range of 3-9 $cm^{-3}s^{-1}$ for different regions[56], while the loss rates of ions of in Beijing was significantly higher than those in clean and rural areas. For instance, the median CS was ~0.016 s^{-1} during NPF periods in Beijing, and those in Hyytiälä[17], Jungfraujoch[18], and Aboa[19] are ~0.002 s^{-1}, ~0.0002 s^{-1}, and ~0.0003 s^{-1}, respectively. Thus, the concentration of large ion clusters in Beijing was much lower than those in clean and rural areas and could not be detected. Similar result was observed in Shanghai[57]. Moreover, ion OOM dimers, whose formation is the first step of OOM clustering[58, 59], were observed during NPF periods in Hyytiälä[17], while not in Beijing, This could be related to the high nitrogen oxides (NOx) levels in urban Beijing, as NOx can terminate the dimerization reactions of peroxy radicals that produce OOM dimers[35, 60]. An evidence is that a large number of organonitrates were observed in Beijing. The absence of OOM dimers is consistent with the low correlations between OOM clusters and sub-3 nm particles in Beijing.

==========

298 Place Figure 3 Here

299 ==========

300 **3.2 Variation of ammonia and amines in ion acid-base clusters**

301 For ion acid-base clusters in urban Beijing, the fraction of amine-containing clusters
302 (f_{amine}) decreased with an increase in the cluster size, i.e., the number of SA molecules,
303 while that of NH_3-containing clusters increased (Fig. 4). Trimer (A_3B_1) is the smallest
304 ion cluster that was detected to contain bases and only amines were observed as the
305 base molecule in them. Trimers containing C_2-amine, C_3-amine, and C_4-amine account
306 for 44.6%, 18.9%, and 36.5%, respectively. For tetramers (A_4B_{1-2}), both amines and
307 NH_3 were observed as the base molecule and their fractions are approximately the
308 same. For pentamers (A_5B_{1-3}), the fraction of SA-amine clusters further decreases to
309 8.5%, while SA-NH_3 and SA-amine-NH_3 clusters account for 54.7% and 13.9%,
310 respectively. For hexamers (A_6B_{2-4}), SA-amine clusters were not observed. SA-NH_3
311 clusters and ion SA-amine-NH_3 clusters account for 66.0% and 34.0%, respectively.
312 The fractions of SA-amine-NH_3 clusters and SA-amine (-NH_3) clusters are divided
313 into the parts contributed by amines and NH_3 based on the number of amine or NH_3
314 molecules in clusters. Thus, the fraction of amine-containing clusters includes the
315 fraction of SA-amine clusters, part fractions of SA-amine-NH_3 clusters, and part
316 fractions of SA-amine (-NH_3) clusters (Eq. S2). A_1, A_2, A_3, and A_4, which do not
317 contain bases, are not included in this analysis.

318 Many kinds of amines, i.e., $C_{1,2,3,4}$-amines, were observed in clusters during NPF in
319 Beijing. Due to high proton affinities, $C_{3,4}$-amines can form monomers and dimers as
320 efficiently as C_2-amines, according to both theoretical and experimental results[27, 61, 62].
321 However, the subsequent cluster formation could be hindered by the steric effect of the
322 alkyl groups in $C_{3,4}$-amines[61]. Results in Beijing showed that all $C_{1,2,3,4}$-amines were
323 observed in the trimers and tetramers, but only $C_{1,2}$-amines were observed in hexamers
324 (Table S1). A possible explanation is that hexamers with $C_{3,4}$-amines are not formed
325 due to the steric effect.

==========

Place Figure 4 Here

==========

In addition to ambient data in Beijing, we also revisited ion acid-base cluster composition from previous CLOUD chamber experiments performed under conditions of various concentrations of NH_3 and DMA[16, 48]. We found that the variation of DMA and NH_3 in ion acid-base clusters with the cluster size is similar to that in Beijing. Specifically, we found that the fraction of DMA-containing clusters (f_{DMA}) all decreased and that of NH_3-containing clusters all increased with the increase in the cluster size with different concentrations of gaseous NH_3 and DMA (Fig. 5). The calculation of f_{DMA} is similar to that of f_{amine} (Eq. S3). The largest clusters observed in CLOUD experiments contained 10 SA molecules, which is larger than that in urban Beijing.

==========

Place Figure 5 Here

==========

Based on the chamber experiments, it is shown that the increasing trend of NH_3-containing clusters is unaffected by the concentrations of gaseous DMA and NH_3 in the tested conditions and could be resulted from the variation of cluster stabilities. It was suggested that the difference between stabilities of NH_3-containing clusters and DMA-containing clusters should decreases with an increase in the cluster size, and theoretical calculation support this. According to the data reported by Myllys et al.[13], the difference of the evaporation rates between SA-NH_3 clusters and SA-DMA clusters is reduced with an increase in the cluster size for both neutral clusters and ion clusters (Fig. S8). According to previous studies, an NH_3 molecule can form more hydrogen bonds (up to 4) than DMA (only two) in clusters; with the increase of cluster size, the stability of SA-NH_3 clusters is enhanced[22, 23]. Flow tube experiments showed that the substitution

rates of NH_3 by DMA in ion acid-base clusters also got slower with the increase in cluster size up to clusters containing 10 SA molecules[24]. Besides cluster stabilities, the high relative abundance of NH_3 to amines also facilitates the involvement of NH_3 in the formation of large clusters (as shown in Figure 5). Thus, the high fraction of NH_3-containing clusters in Beijing could result from both the high abundance of NH_3 and the increased cluster stability of NH_3-containing in large sizes. Furtherly, simulation of neutral cluster formation of SA, DMA, and NH_3 under atmospheric conditions of urban Beijing showed that NH_3 got involved little in forming monomer and dimer but evidently contributed to the formation of larger clusters such as tetramers (Fig. S9). A recent study at the same site in urban Beijing showed that NH_3 was more abundant than amines in ultrafine particles[63].

3.3 Average base number of ion acid-base clusters

In addition to the relative contribution, the ABN of NH_3 (m_{NH3}) of ion acid-base clusters also increased significantly with an increase in the cluster size, but the ABN of amine (m_{amine}) showed a different trend (Fig. 6a). The ABN of ion acid-base clusters in Beijing includes two parts, m_{NH3} and m_{amine}, and they both increased with an increase in the cluster size, consistent with the adding of base molecules along with clustering growth. However, in different stages, the added numbers of NH_3 and amines molecules are different. For trimers, m_{amine} dominates the ABN, with m_{NH3} being zero and m_{amine} being 0.024, respectively. However, as the cluster size increases, m_{NH3} increases more rapidly than m_{amine}, consistent with the increasing faction of NH_3-containing clusters. When the number of SA molecules is 6, m_{NH3} is 2.66 and m_{amine} is only 0.51. The ABN of ion acid-base clusters observed in different days does not change much (Fig. S10). In CLOUD chamber experiments, the ABN_6 of SA-DMA clusters was between 4.5~4.8, and that of SA-NH_3 clusters was between 0~3.0 (Fig. 6a). In clean atmospheric environments such as Hyytiälä, Jungfraujoch, and Aboa, the ABN_6 of ion acid-base clusters, which is actually m_{NH3}, observed during NPF periods is 3.16, 2.28, and 1.80, respectively (Fig. 6b).

==========

Place Figure 6 Here

==========

The differences in ABN values among different environments or experiments are governed by the ratio of gaseous base concentrations to acid concentrations ([DMA]/[SA] ratio or [NH_3]/[SA] ratio). High [NH_3]/[SA] ratio leads to high ABN of SA-NH_3 clusters, according to both model simulations and chamber experiments[46, 64]. It should be similar for SA-DMA clusters, as shown in Figure S11. During the measurement, the [DMA]/[SA] ratio and [NH_3]/[SA] ratio in Beijing are calculated by using the median concentrations of DMA, NH_3 and SA during NPF periods measured at the same site, i.e., 1.8 pptv[65], 789 pptv[65] and 2.6×10^6 cm^{-3} (0.10 pptv), respectively. In urban Beijing, the [DMA]/[SA] ratio (18.2) was lower than that used in CLOUD experiments (52.8 – 1325), resulting in the much lower m_{amine} in Beijing. Meanwhile, the [NH_3]/[SA] ratio (8100) in urban Beijing was higher than that used in CLOUD experiments (1.62 – 109)[16], as a result, m_{NH3} in Beijing was higher (as shown in Fig. S11b). Actually, ABN increases little when the [NH_3]/[SA] ratio is higher than a threshold value of ~30 (Fig. S11). The same also applies to the case of SA-DMA clustering. The [DMA]/[SA] ratios in CLOUD experiments seemed to be always above the threshold value, and thus, the ABN of SA-DMA clusters did not change much. The saturated DMA concentration for SA-DMA nucleation was reported to be approximately 5 pptv in a CLOUD chamber study[16], much higher than their concentration observed during NPF periods in urban Beijing. In addition, the sequence of ABN in Hyytiälä, Jungfraujoch, and Aboa is consistent with the concentration of their gaseous precursors, especially those of base molecules. Their ABN values are lower than those in urban Beijing and close to those of ion SA-NH_3 clusters in CLOUD experiments. In Hyytiälä, Jungfraujoch, and Aboa, the concentrations of NH_3 were between 0.0021~3.4 ppbv, below 1 ppbv, and between 0.001~1 ppbv, respectively[18, 19, 66], which were much lower than the concentration of NH_3 in Beijing. In addition to

precursor concentrations, stability of clusters which changes with temperature is another factor that affects ABN. In this study, the temperatures of CLOUD experiments, Beijing, and Hyytiälä[17] are all around 278K, while those of Aboa[19] and Jungfraujoch[18] are approximately 15K lower. The lower temperature would lead to higher ABN[46, 64], however, the ABN in Aboa and Jungfraujoch are still lower than that in Beijing and Hyytiälä. Therefore, these reflect the significant influence of gaseous precursors on ABN at these four sites in comparison to the temperature.

4 Implications

Simultaneous measurements of atmospheric ion clusters and neutral clusters reveal the relatively comprehensive composition of key clusters and precursors contributing to NPF in urban Beijing. Previous study of Cai et al.[65] indicated that clusters were initially formed by SA and amine molecules during NPF periods in Beijing. Our results are consistent and further suggested that NH_3 plays an important role in the formation of large clusters in Beijing. This is distinct from that in clean and rural areas because in the urban atmosphere, there are adequate amines which are mainly from anthropogenic emissions[67]. However, the abundance of gaseous amines in urban Beijing (~ 1.8 pptv during NPF periods[36]) are not high enough to saturate SA-amine clustering such that NH_3 plays its role in the following growth of large clusters, especially when the concentration of NH_3 is at ppbv-level (~ 789 pptv during NPF periods[36]). Results from both controlled experiments and theoretical calculations indicated the increasing ability of NH_3 to form acid-base clusters with the increase of cluster size. In the meanwhile, for other urban atmospheres, which contain ppbv-level NH_3 and a few pptv amines, the clustering pathway could be similar.

As potential precursors, OOMs have been reported to contribute to the clustering in clean and rural areas such as Hyytiälä[17] and Jungfraujoch[18], however, they took little part in the clustering process in urban Beijing. The median OOM concentration in urban Beijing was about 3×10^7 cm^{-3} during our measurement[60]. With such an abundance, the particle formation rates of either BioOxOrg clustering[59], SA-BioOxOrg clustering[34], or

SA-BioOxOrg-NH_3 clustering[35] will be below 10 $cm^{-3}s^{-1}$, which are much lower than those of SA-DMA clustering[16] and the measured formation rates in urban Beijing[36]. Moreover, the formation of OOMs dimers which facilitate particle formation[35] was probably suppressed by high NOx here[35] as many organonitrates were observed instead of them. Nevertheless, OOMs can play an important role in the growth of newly formed nanoparticles[60] in urban Beijing as they condense more readily on particles as the particles grow.

The observed acid-base cluster composition may not fully represent the clustering pathway. For example, NH_3 may get involved in the cluster formation but then be substituted by amines in clusters[26, 27], and NH_3 is more easily to escape from clusters than amines during the measurement. Thus, the actual participation of NH_3 in the clustering processes could be higher than observed here.

Supplementary Information

The Supplementary Information include the calculation of the CS (Eq. S1); The calculation of the fraction of amine-containing clusters and DMA-containing clusters (Eq. S2 and Eq. S3); Formulas of acid-base ion clusters observed in Beijing (Table S1); Conditions of three CLOUD experiments as illustrated in Figure 5 (Table S2); The relative transmission efficiency curves of mass spectrometer (Figure S1); Comparison of neutral clusters between Beijing and Shanghai (Figure S2); Particle size distributions, the composition of ion clusters and neutral clusters during non-NPF periods in urban Beijing (Figure S3); Correlations of acid-base clusters and OOMs with sub-3 nm particles (Figures S4 and S5); Particle size distributions, cluster composition, and their time series during Nov. 2018 (Figures S6 and S7); Evaporation rates of acid-base clusters (Figure S8); Simulated cluster formation under atmospheric conditions of Beijing (Figure S9); ABN of acid-base ion clusters during different NPF periods in Beijing (Figure S10); ABN of SA-DMA ion clusters and SA-NH_3 ion clusters observed in CLOUD experimental conditions (Figure S11).

Acknowledgement

Financial support from National Natural Science Foundation of China (21876094, 41730106, and 92044301) and Samsung $PM_{2.5}$ SRP is acknowledged. We thank the CLOUD team for sharing their published experimental data.

Corresponding Author

Jingkun Jiang (jiangjk@tsinghua.edu.cn)

Reference

1. Merikanto, J.; Spracklen, D. V.; Mann, G. W.; Pickering, S. J.; Carslaw, K. S. Impact of nucleation on global CCN. *Atmos. Chem. Phys.* **2009,** *9* (21), 8601-8616.

2. Zhang, R.; Khalizov, A.; Wang, L.; Hu, M.; Xu, W. Nucleation and growth of nanoparticles in the atmosphere. *Chem. Rev.* **2012,** *112* (3), 1957-2011.

3. Schobesberger, S.; Junninen, H.; Bianchi, F.; Lonn, G.; Ehn, M.; Lehtipalo, K.; Dommen, J.; Ehrhart, S.; Ortega, I. K.; Franchin, A.; Nieminen, T.; Riccobono, F.; Hutterli, M.; Duplissy, J.; Almeida, J.; Amorim, A.; Breitenlechner, M.; Downard, A. J.; Dunne, E. M.; Flagan, R. C.; Kajos, M.; Keskinen, H.; Kirkby, J.; Kupc, A.; Kurten, A.; Kurten, T.; Laaksonen, A.; Mathot, S.; Onnela, A.; Praplan, A. P.; Rondo, L.; Santos, F. D.; Schallhart, S.; Schnitzhofer, R.; Sipila, M.; Tome, A.; Tsagkogeorgas, G.; Vehkamaki, H.; Wimmer, D.; Baltensperger, U.; Carslaw, K. S.; Curtius, J.; Hansel, A.; Petaja, T.; Kulmala, M.; Donahue, N. M.; Worsnop, D. R. Molecular understanding of atmospheric particle formation from sulfuric acid and large oxidized organic molecules. *Proc. Natl. Acad. Sci. U. S. A.* **2013,** *110* (43), 17223-17228.

4. Lehtipalo, K.; Rondo, L.; Kontkanen, J.; Schobesberger, S.; Jokinen, T.; Sarnela, N.; Kurten, A.; Ehrhart, S.; Franchin, A.; Nieminen, T.; Riccobono, F.; Sipila, M.; Yli-Juuti, T.; Duplissy, J.; Adamov, A.; Ahlm, L.; Almeida, J.; Amorim, A.; Bianchi, F.; Breitenlechner, M.; Dommen, J.; Downard, A. J.; Dunne, E. M.; Flagan, R. C.; Guida, R.; Hakala, J.; Hansel, A.; Jud, W.; Kangasluoma, J.; Kerminen, V. M.; Keskinen, H.; Kim, J.; Kirkby, J.; Kupc, A.; Kupiainen-Maatta, O.; Laaksonen, A.; Lawler, M. J.; Leiminger, M.; Mathot, S.; Olenius, T.; Ortega, I. K.; Onnela, A.; Petaja, T.; Praplan, A.; Rissanen, M. P.; Ruuskanen, T.; Santos, F. D.; Schallhart, S.; Schnitzhofer, R.; Simon, M.; Smith, J. N.; Trostl, J.; Tsagkogeorgas, G.; Tome, A.; Vaattovaara, P.; Vehkamaki, H.; Vrtala, A. E.; Wagner, P. E.; Williamson, C.; Wimmer, D.; Winkler, P. M.; Virtanen, A.; Donahue, N. M.; Carslaw, K. S.; Baltensperger, U.; Riipinen, I.; Curtius, J.; Worsnop, D. R.; Kulmala, M. The effect of acid-base clustering and ions on the growth of atmospheric nano-particles. *Nat. Commun.* **2016,** *7*, 11594.

5. Jokinen, T.; Sipilä, M.; Junninen, H.; Ehn, M.; Lönn, G.; Hakala, J.; Petäjä, T.; Mauldin, R. L.; Kulmala, M.; Worsnop, D. R. Atmospheric sulphuric acid and neutral cluster measurements using CI-APi-TOF. *Atmos. Chem. Phys.* **2012,** *12* (9), 4117-4125.

6. Zhao, J.; Eisele, F. L.; Titcombe, M.; Kuang, C.; McMurry, P. H. Chemical ionization mass spectrometric measurements of atmospheric neutral clusters using the cluster-CIMS. *J. Geophys. Res.* **2010,** *115*, D08205.

7. Hanson, D. R. Measurement of prenucleation molecular clusters in the NH_3, H_2SO_4, H_2O system. *J. Geophys. Res.* **2002,** *107* (D12), AAC10-1-18.
8. Ortega, I. K.; Olenius, T.; Kupiainen-Määttä, O.; Loukonen, V.; Kurtén, T.; Vehkamäki, H. Electrical charging changes the composition of sulfuric acid–ammonia/dimethylamine clusters. *Atmos. Chem. Phys.* **2014,** *14* (15), 7995-8007.
9. Junninen, H.; Ehn, M.; Petäjä, T.; Luosujärvi, L.; Kotiaho, T.; Kostiainen, R.; Rohner, U.; Gonin, M.; Fuhrer, K.; Kulmala, M.; Worsnop, D. R. A high-resolution mass spectrometer to measure atmospheric ion composition. *Atmos. Meas. Tech.* **2010,** *3* (4), 1039-1053.
10. Ehn, M.; Junninen, H.; J, T. P.; Kurtén, T.; Kerminen, V. M.; Schobesberger, S.; Manninen, H. E.; Ortega, I. K.; Ki, H. V.; Kulmala, M. Composition and temporal behavior of ambient ions in the boreal forest. *Atmos. Chem. Phys.* **2010,** *10* (17), 768-773.
11. Kirkby, J.; Curtius, J.; Almeida, J.; Dunne, E.; Duplissy, J.; Ehrhart, S.; Franchin, A.; Gagné, S.; Ickes, L.; Kürten, A. Role of sulphuric acid, ammonia and galactic cosmic rays in atmospheric aerosol nucleation. *Nature* **2011,** *476* (7361), 429.
12. Ortega, I. K.; Kupiainen, O.; Kurtén, T.; Olenius, T.; Wilkman, O.; McGrath, M. J.; Loukonen, V.; Vehkamäki, H. From quantum chemical formation free energies to evaporation rates. *Atmos. Chem. Phys.* **2012,** *12* (1), 225-235.
13. Myllys, N.; Kubečka, J.; Besel, V.; Alfaouri, D.; Olenius, T.; Smith, J. N.; Passananti, M. Role of base strength, cluster structure and charge in sulfuric-acid-driven particle formation. *Atmos. Chem. Phys.* **2019,** *19* (15), 9753-9768.
14. Kurtén, T.; Loukonen, V.; Vehkam?ki, H.; Kulmala, M. Amines are likely to enhance neutral and ion-induced sulfuric acid-water nucleation in the atmosphere more effectively than ammonia. *Atmos. Chem. Phys.* **2008,** *8* (14), 7455-7476.
15. Kürten, A.; Jokinen, T.; Simon, M.; Sipilä, M.; Sarnela, N.; Junninen, H.; Adamov, A.; Almeida, J.; Amorim, A.; Bianchi, F. Neutral molecular cluster formation of sulfuric acid-dimethylamine observed in real time under atmospheric conditions. *Proc. Natl. Acad. Sci. U. S. A.* **2014,** *111* (42), 15019-15024.
16. Almeida, J.; Schobesberger, S.; Kurten, A.; Ortega, I. K.; Kupiainen-Maatta, O.; Praplan, A. P.; Adamov, A.; Amorim, A.; Bianchi, F.; Breitenlechner, M.; David, A.; Dommen, J.; Donahue, N. M.; Downard, A.; Dunne, E.; Duplissy, J.; Ehrhart, S.; Flagan, R. C.; Franchin, A.; Guida, R.; Hakala, J.; Hansel, A.; Heinritzi, M.; Henschel, H.; Jokinen, T.; Junninen, H.; Kajos, M.; Kangasluoma, J.; Keskinen, H.; Kupc, A.; Kurten, T.; Kvashin, A. N.; Laaksonen, A.; Lehtipalo, K.; Leiminger, M.; Leppa, J.; Loukonen, V.; Makhmutov, V.; Mathot, S.; McGrath, M. J.; Nieminen, T.; Olenius, T.; Onnela, A.; Petaja, T.; Riccobono, F.; Riipinen, I.; Rissanen, M.; Rondo, L.; Ruuskanen, T.; Santos, F. D.; Sarnela, N.; Schallhart, S.; Schnitzhofer, R.; Seinfeld, J. H.; Simon, M.; Sipila, M.; Stozhkov, Y.; Stratmann, F.; Tome, A.; Trostl, J.; Tsagkogeorgas, G.; Vaattovaara, P.; Viisanen, Y.; Virtanen, A.; Vrtala, A.; Wagner, P. E.; Weingartner, E.; Wex, H.; Williamson, C.; Wimmer, D.; Ye, P.; Yli-Juuti, T.; Carslaw, K. S.; Kulmala, M.; Curtius, J.; Baltensperger, U.; Worsnop, D. R.; Vehkamaki, H.; Kirkby, J. Molecular understanding of sulphuric acid-amine particle nucleation in the atmosphere. *Nature* **2013,** *502* (7471), 359-363.
17. Yan, C.; Dada, L.; Rose, C.; Jokinen, T.; Nie, W.; Schobesberger, S.; Junninen, H.; Lehtipalo, K.; Sarnela, N.; Makkonen, U.; Garmash, O.; Wang, Y.; Zha, Q.; Paasonen, P.; Bianchi, F.; Sipilä, M.; Ehn, M.; Petäjä, T.; Kerminen, V.-M.; Worsnop, D. R.; Kulmala, M. The role of H2SO4-NH3 anion clusters in ion-induced aerosol nucleation mechanisms in the boreal forest. *Atmos. Chem. Phys.* **2018,** *18* (17), 13231-13243.
18. Bianchi, F.; Trostl, J.; Junninen, H.; Frege, C.; Henne, S.; Hoyle, C. R.; Molteni, U.; Herrmann, E.;

Adamov, A.; Bukowiecki, N.; Chen, X.; Duplissy, J.; Gysel, M.; Hutterli, M.; Kangasluoma, J.; Kontkanen, J.; Kurten, A.; Manninen, H. E.; Munch, S.; Perakyla, O.; Petaja, T.; Rondo, L.; Williamson, C.; Weingartner, E.; Curtius, J.; Worsnop, D. R.; Kulmala, M.; Dommen, J.; Baltensperger, U. New particle formation in the free troposphere: A question of chemistry and timing. *Science* **2016,** *352* (6289), 1109-1112.

19. Jokinen, T.; Sipila, M.; Kontkanen, J.; Vakkari, V.; Tisler, P.; Duplissy, E. M.; Junninen, H.; Kangasluoma, J.; Manninen, H. E.; Petaja, T.; Kulmala, M.; Worsnop, D. R.; Kirkby, J.; Virkkula, A.; Kerminen, V. M. Ion-induced sulfuric acid-ammonia nucleation drives particle formation in coastal Antarctica. *Sci. Adv.* **2018,** *4* (11), eaat9744.

20. Yao, L.; Garmash, O.; Bianchi, F.; Zheng, J.; Yan, C.; Kontkanen, J.; Junninen, H.; Mazon, S. B.; Ehn, M.; Paasonen, P.; Sipila, M.; Wang, M. Y.; Wang, X. K.; Xiao, S.; Chen, H. F.; Lu, Y. Q.; Zhang, B. W.; Wang, D. F.; Fu, Q. Y.; Geng, F. H.; Li, L.; Wang, H. L.; Qiao, L. P.; Yang, X.; Chen, J. M.; Kerminen, V. M.; Petaja, T.; Worsnop, D. R.; Kulmala, M.; Wang, L. Atmospheric new particle formation from sulfuric acid and amines in a Chinese megacity. *Science* **2018,** *361* (6399), 278-281.

21. Myllys, N.; Chee, S.; Olenius, T.; Lawler, M.; Smith, J. Molecular-Level Understanding of Synergistic Effects in Sulfuric Acid-Amine-Ammonia Mixed Clusters. *J. Phys. Chem. A* **2019,** *123* (12), 2420-2425.

22. Bzdek, B. R.; DePalma, J. W.; Johnston, M. V. Mechanisms of Atmospherically Relevant Cluster Growth. *Acc. Chem. Res.* **2017,** *50* (8), 1965-1975.

23. DePalma, J. W.; Bzdek, B. R.; Doren, D. J.; Johnston, M. V. Structure and Energetics of Nanometer Size Clusters of Sulfuric Acid with Ammonia and Dimethylamine. *J. Phys. Chem. A* **2012,** *116* (3), 1030-1040.

24. Bzdek, B. R.; DePalma, J. W.; Johnston, M. V. Mechanisms of Atmospherically Relevant Cluster Growth. *Acc. Chem. Res.* **2017,** *50* (8), 1965-1975.

25. Lawler, M. J.; Winkler, P. M.; Kim, J.; Ahlm, L.; Tröstl, J.; Praplan, A. P.; Schobesberger, S.; Kürten, A.; Kirkby, J.; Bianchi, F.; Duplissy, J.; Hansel, A.; Jokinen, T.; Keskinen, H.; Lehtipalo, K.; Leiminger, M.; Petäjä, T.; Rissanen, M.; Rondo, L.; Simon, M.; Sipilä, M.; Williamson, C.; Wimmer, D.; Riipinen, I.; Virtanen, A.; Smith, J. N. Unexpectedly acidic nanoparticles formed in dimethylamine–ammonia–sulfuric-acid nucleation experiments at CLOUD. *Atmos. Chem. Phys.* **2016,** *16* (21), 13601-13618.

26. Li, H.; Ning, A.; Zhong, J.; Zhang, H.; Liu, L.; Zhang, Y.; Zhang, X.; Zeng, X. C.; He, H. Influence of atmospheric conditions on sulfuric acid-dimethylamine-ammonia-based new particle formation. *Chemosphere* **2020,** *245*, 125554.

27. Glasoe, W. A.; Volz, K.; Panta, B.; Freshour, N.; Bachman, R.; Hanson, D. R.; McMurry, P. H.; Jen, C. Sulfuric acid nucleation: An experimental study of the effect of seven bases. *J. Geophys. Res.: Atmos.* **2015,** *120* (5), 1933-1950.

28. Jen, C. N.; McMurry, P. H.; Hanson, D. R. Stabilization of sulfuric acid dimers by ammonia, methylamine, dimethylamine, and trimethylamine. *J Geophys Res-Atmos* **2014,** *119* (12), 7502-7514.

29. Olenius, T.; Halonen, R.; Kurtén, T.; Henschel, H.; Kupiainen-Määttä, O.; Ortega, I. K.; Jen, C. N.; Vehkamäki, H.; Riipinen, I. New particle formation from sulfuric acid and amines: Comparison of monomethylamine, dimethylamine, and trimethylamine. *J. Geophys. Res.: Atmos.* **2017,** *122* (13), 7103-7118.

30. Zheng, J.; Ma, Y.; Chen, M.; Zhang, Q.; Wang, L.; Khalizov, A. F.; Yao, L.; Wang, Z.; Wang, X.; Chen, L. Measurement of atmospheric amines and ammonia using the high resolution time-of-flight chemical ionization mass spectrometry. *Atmos. Environ.* **2015,** *102*, 249-259.

31. Yao, L.; Wang, M.-Y.; Wang, X.-K.; Liu, Y.-J.; Chen, H.-F.; Zheng, J.; Nie, W.; Ding, A.-J.; Geng, F.-H.; Wang, D.-F.; Chen, J.-M.; Worsnop, D. R.; Wang, L. Detection of atmospheric gaseous amines and amides by a high-resolution time-of-flight chemical ionization mass spectrometer with protonated ethanol reagent ions. *Atmos. Chem. Phys.* **2016,** *16* (22), 14527-14543.
32. Wu, R.; Bo, Y.; Li, J.; Li, L.; Li, Y.; Xie, S. Method to establish the emission inventory of anthropogenic volatile organic compounds in China and its application in the period 2008–2012. *Atmos. Environ.* **2016,** *127*, 244-254.
33. Kirkby, J.; Duplissy, J.; Sengupta, K.; Frege, C.; Gordon, H.; Williamson, C.; Heinritzi, M.; Simon, M.; Yan, C.; Almeida, J.; Trostl, J.; Nieminen, T.; Ortega, I. K.; Wagner, R.; Adamov, A.; Amorim, A.; Bernhammer, A. K.; Bianchi, F.; Breitenlechner, M.; Brilke, S.; Chen, X.; Craven, J.; Dias, A.; Ehrhart, S.; Flagan, R. C.; Franchin, A.; Fuchs, C.; Guida, R.; Hakala, J.; Hoyle, C. R.; Jokinen, T.; Junninen, H.; Kangasluoma, J.; Kim, J.; Krapf, M.; Kurten, A.; Laaksonen, A.; Lehtipalo, K.; Makhmutov, V.; Mathot, S.; Molteni, U.; Onnela, A.; Perakyla, O.; Piel, F.; Petaja, T.; Praplan, A. P.; Pringle, K.; Rap, A.; Richards, N. A.; Riipinen, I.; Rissanen, M. P.; Rondo, L.; Sarnela, N.; Schobesberger, S.; Scott, C. E.; Seinfeld, J. H.; Sipila, M.; Steiner, G.; Stozhkov, Y.; Stratmann, F.; Tome, A.; Virtanen, A.; Vogel, A. L.; Wagner, A. C.; Wagner, P. E.; Weingartner, E.; Wimmer, D.; Winkler, P. M.; Ye, P.; Zhang, X.; Hansel, A.; Dommen, J.; Donahue, N. M.; Worsnop, D. R.; Baltensperger, U.; Kulmala, M.; Carslaw, K. S.; Curtius, J. Ion-induced nucleation of pure biogenic particles. *Nature* **2016,** *533* (7604), 521-526.
34. Riccobono, F.; Schobesberger, S.; Scott, C. E.; Dommen, J.; Ortega, I. K.; Rondo, L.; Almeida, J.; Amorim, A.; Bianchi, F.; Breitenlechner, M.; David, A.; Downard, A.; Dunne, E. M.; Duplissy, J.; Ehrhart, S.; Flagan, R. C.; Franchin, A.; Hansel, A.; Junninen, H.; Kajos, M.; Keskinen, H.; Kupc, A.; Kurten, A.; Kvashin, A. N.; Laaksonen, A.; Lehtipalo, K.; Makhmutov, V.; Mathot, S.; Nieminen, T.; Onnela, A.; Petaja, T.; Praplan, A. P.; Santos, F. D.; Schallhart, S.; Seinfeld, J. H.; Sipila, M.; Spracklen, D. V.; Stozhkov, Y.; Stratmann, F.; Tome, A.; Tsagkogeorgas, G.; Vaattovaara, P.; Viisanen, Y.; Vrtala, A.; Wagner, P. E.; Weingartner, E.; Wex, H.; Wimmer, D.; Carslaw, K. S.; Curtius, J.; Donahue, N. M.; Kirkby, J.; Kulmala, M.; Worsnop, D. R.; Baltensperger, U. Oxidation products of biogenic emissions contribute to nucleation of atmospheric particles. *Science* **2014,** *344* (6185), 717-721.
35. Lehtipalo, K.; Yan, C.; Dada, L.; Bianchi, F.; Xiao, M.; Wagner, R.; Stolzenburg, D.; Ahonen, L. R.; Amorim, A.; Baccarini, A.; Bauer, P. S.; Baumgartner, B.; Bergen, A.; Bernhammer, A. K.; Breitenlechner, M.; Brilke, S.; Buchholz, A.; Mazon, S. B.; Chen, D. X.; Chen, X. M.; Dias, A.; Dommen, J.; Draper, D. C.; Duplissy, J.; Ehn, M.; Finkenzeller, H.; Fischer, L.; Frege, C.; Fuchs, C.; Garmash, O.; Gordon, H.; Hakala, J.; He, X. C.; Heikkinen, L.; Heinritzi, M.; Helm, J. C.; Hofbauer, V.; Hoyle, C. R.; Jokinen, T.; Kangasluoma, J.; Kerminen, V. M.; Kim, C.; Kirkby, J.; Kontkanen, J.; Kurten, A.; Lawler, M. J.; Mai, H. J.; Mathot, S.; Mauldin, R. L.; Molteni, U.; Nichman, L.; Nie, W.; Nieminen, T.; Ojdanic, A.; Onnela, A.; Passananti, M.; Petaja, T.; Piel, F.; Pospisilova, V.; Quelever, L. L. J.; Rissanen, M. P.; Rose, C.; Sarnela, N.; Schallhart, S.; Schuchmann, S.; Sengupta, K.; Simon, M.; Sipila, M.; Tauber, C.; Tome, A.; Trostl, J.; Vaisanen, O.; Vogel, A. L.; Volkamer, R.; Wagner, A. C.; Wang, M. Y.; Weitz, L.; Wimmer, D.; Ye, P. L.; Ylisirnio, A.; Zha, Q. Z.; Carslaw, K. S.; Curtius, J.; Donahue, N. M.; Flagan, R. C.; Hansel, A.; Riipinen, I.; Virtanen, A.; Winkler, P. M.; Baltensperger, U.; Kulmala, M.; Worsnop, D. R. Multicomponent new particle formation from sulfuric acid, ammonia, and biogenic vapors. *Sci. Adv.* **2018,** *4* (12), eaau5363.
36. Deng, C.; Fu, Y.; Dada, L.; Yan, C.; Cai, R.; Yang, D.; Zhou, Y.; Yin, R.; Lu, Y.; Li, X.; Qiao, X.; Fan, X.; Nie, W.; Kontkanen, J.; Kangasluoma, J.; Chu, B.; Ding, A.; Kerminen, V. M.; Paasonen, P.; Worsnop, D. R.; Bianchi, F.; Liu, Y.; Zheng, J.; Wang, L.; Kulmala, M.; Jiang, J. Seasonal Characteristics

of New Particle Formation and Growth in Urban Beijing. *Environ. Sci. Technol.* **2020,** *54* (14), 8547-8557.
37. Liu, Y.; Yan, C.; Feng, Z.; Zheng, F.; Fan, X.; Zhang, Y.; Li, C.; Zhou, Y.; Lin, Z.; Guo, Y.; Zhang, Y.; Ma, L.; Zhou, W.; Liu, Z.; Dada, L.; Dällenbach, K.; Kontkanen, J.; Cai, R.; Chan, T.; Chu, B.; Du, W.; Yao, L.; Wang, Y.; Cai, J.; Kangasluoma, J.; Kokkonen, T.; Kujansuu, J.; Rusanen, A.; Deng, C.; Fu, Y.; Yin, R.; Li, X.; Lu, Y.; Liu, Y.; Lian, C.; Yang, D.; Wang, W.; Ge, M.; Wang, Y.; Worsnop, D. R.; Junninen, H.; He, H.; Kerminen, V.-M.; Zheng, J.; Wang, L.; Jiang, J.; Petäjä, T.; Bianchi, F.; Kulmala, M. Continuous and comprehensive atmospheric observations in Beijing: a station to understand the complex urban atmospheric environment. *Big Earth Data* **2020,** *4* (3), 295-321.
38. Li, X.; Zhao, B.; Zhou, W.; Shi, H.; Yin, R.; Cai, R.; Yang, D.; Dallenbach, K.; Deng, C.; Fu, Y.; Qiao, X.; Wang, L.; Liu, Y.; Yan, C.; Kulmala, M.; Zheng, J.; Hao, J.; Wang, S.; Jiang, J. Responses of gaseous sulfuric acid and particulate sulfate to reduced SO_2 concentration: A perspective from long-term measurements in Beijing. *Sci. Total Environ.* **2020,** *721*, 137700.
39. Lu, Y.; Yan, C.; Fu, Y.; Chen, Y.; Liu, Y.; Yang, G.; Wang, Y.; Bianchi, F.; Chu, B.; Zhou, Y.; Yin, R.; Baalbaki, R.; Garmash, O.; Deng, C.; Wang, W.; Liu, Y.; Petäjä, T.; Kerminen, V.-M.; Jiang, J.; Kulmala, M.; Wang, L. A proxy for atmospheric daytime gaseous sulfuric acid concentration in urban Beijing. *Atmos. Chem. Phys.* **2019,** *19* (3), 1971-1983.
40. Kurten, A.; Rondo, L.; Ehrhart, S.; Curtius, J. Calibration of a chemical ionization mass spectrometer for the measurement of gaseous sulfuric acid. *J. Phys. Chem. A* **2012,** *116* (24), 6375-86.
41. Heinritzi, M.; Simon, M.; Steiner, G.; Wagner, A. C.; Kürten, A.; Hansel, A.; Curtius, J. Characterization of the mass-dependent transmission efficiency of a CIMS. *Atmos. Meas. Tech.* **2016,** *9* (4), 1449-1460.
42. Jiang, J.; Chen, M.; Kuang, C.; Attoui, M.; McMurry, P. H. Electrical Mobility Spectrometer Using a Diethylene Glycol Condensation Particle Counter for Measurement of Aerosol Size Distributions Down to 1 nm. *Aerosol Sci. Technol.* **2011,** *45* (4), 510-521.
43. Cai, R.; Chen, D.-R.; Hao, J.; Jiang, J. A miniature cylindrical differential mobility analyzer for sub-3 nm particle sizing. *J. Aerosol Sci* **2017,** *106*, 111-119.
44. Liu, J. Q.; Jiang, J. K.; Zhang, Q.; Deng, J. G.; Hao, J. M. A spectrometer for measuring particle size distributions in the range of 3 nm to 10 mu m. *Front. Environ. Sci. Eng.* **2016,** *10* (1), 63-72.
45. Fu, Y.; Xue, M.; Cai, R.; Kangasluoma, J.; Jiang, J. Theoretical and experimental analysis of the core sampling method: Reducing diffusional losses in aerosol sampling line. *Aerosol Sci. Technol.* **2019,** *53* (7), 793-801.
46. Schobesberger, S.; Franchin, A.; Bianchi, F.; Rondo, L.; Duplissy, J.; Kürten, A.; Ortega, I. K.; Metzger, A.; Schnitzhofer, R.; Almeida, J.; Amorim, A.; Dommen, J.; Dunne, E. M.; Ehn, M.; Gagné, S.; Ickes, L.; Junninen, H.; Hansel, A.; Kerminen, V. M.; Kirkby, J.; Kupc, A.; Laaksonen, A.; Lehtipalo, K.; Mathot, S.; Onnela, A.; Petäjä, T.; Riccobono, F.; Santos, F. D.; Sipilä, M.; Tomé, A.; Tsagkogeorgas, G.; Viisanen, Y.; Wagner, P. E.; Wimmer, D.; Curtius, J.; Donahue, N. M.; Baltensperger, U.; Kulmala, M.; Worsnop, D. R. On the composition of ammonia–sulfuric-acid ion clusters during aerosol particle formation. *Atmos. Chem. Phys.* **2015,** *15* (1), 55-78.
47. Waller, S. E.; Yang, Y.; Castracane, E.; Racow, E. E.; Kreinbihl, J. J.; Nickson, K. A.; Johnson, C. J. The Interplay Between Hydrogen Bonding and Coulombic Forces in Determining the Structure of Sulfuric Acid-Amine Clusters. *J. Phys. Chem. Lett.* **2018,** *9* (6), 1216-1222.
48. Bianchi, F.; Praplan, A. P.; Sarnela, N.; Dommen, J.; Kurten, A.; Ortega, I. K.; Schobesberger, S.; Junninen, H.; Simon, M.; Trostl, J.; Jokinen, T.; Sipila, M.; Adamov, A.; Amorim, A.; Almeida, J.;

676 Breitenlechner, M.; Duplissy, J.; Ehrhart, S.; Flagan, R. C.; Franchin, A.; Hakala, J.; Hansel, A.; Heinritzi,
677 M.; Kangasluoma, J.; Keskinen, H.; Kim, J.; Kirkby, J.; Laaksonen, A.; Lawler, M. J.; Lehtipalo, K.;
678 Leiminger, M.; Makhmutov, V.; Mathot, S.; Onnela, A.; Petaja, T.; Riccobono, F.; Rissanen, M. P.; Rondo,
679 L.; Tome, A.; Virtanen, A.; Viisanen, Y.; Williamson, C.; Wimmer, D.; Winkler, P. M.; Ye, P.; Curtius, J.;
680 Kulmala, M.; Worsnop, D. R.; Donahue, N. M.; Baltensperger, U. Insight into acid-base nucleation
681 experiments by comparison of the chemical composition of positive, negative, and neutral clusters.
682 *Environ. Sci. Technol.* **2014,** *48* (23), 13675-13684.
683 49. Bianchi, F.; Garmash, O.; He, X.; Yan, C.; Iyer, S.; Rosendahl, I.; Xu, Z.; Rissanen, M. P.; Riva, M.;
684 Taipale, R.; Sarnela, N.; Petäjä, T.; Worsnop, D. R.; Kulmala, M.; Ehn, M.; Junninen, H. The role of
685 highly oxygenated molecules (HOMs) in determining the composition of ambient ions in the boreal
686 forest. *Atmos. Chem. Phys.* **2017,** *17* (22), 13819-13831.
687 50. Bertram, T. H.; Kimmel, J. R.; Crisp, T. A.; Ryder, O. S.; Yatavelli, R. L. N.; Thornton, J. A.;
688 Cubison, M. J.; Gonin, M.; Worsnop, D. R. A field-deployable, chemical ionization time-of-flight mass
689 spectrometer. *Atmos. Meas. Tech.* **2011,** *4* (7), 1471-1479.
690 51. Cai, R.; Yang, D.; Fu, Y.; Wang, X.; Li, X.; Ma, Y.; Hao, J.; Zheng, J.; Jiang, J. Aerosol surface area
691 concentration: a governing factor in new particle formation in Beijing. *Atmos. Chem. Phys.* **2017,** *17* (20),
692 12327-12340.
693 52. Passananti, M.; Zapadinsky, E.; Zanca, T.; Kangasluoma, J.; Myllys, N.; Rissanen, M. P.; Kurten,
694 T.; Ehn, M.; Attoui, M.; Vehkamaki, H. How well can we predict cluster fragmentation inside a mass
695 spectrometer? *Chem. Commun.* **2019,** *55* (42), 5946-5949.
696 53. Kupiainen, O.; Ortega, I. K.; Kurtén, T.; Vehkamäki, H. Amine substitution into sulfuric acid –
697 ammonia clusters. *Atmos. Chem. Phys.* **2012,** *12* (8), 3591-3599.
698 54. Olenius, T.; Kupiainen-Maatta, O.; Ortega, I. K.; Kurten, T.; Vehkamaki, H. Free energy barrier in
699 the growth of sulfuric acid-ammonia and sulfuric acid-dimethylamine clusters. *J. Chem. Phys.* **2013,** *139*
700 (8), 084312.
701 55. Kirkby, J.; Curtius, J.; Almeida, J.; Dunne, E.; Duplissy, J.; Ehrhart, S.; Franchin, A.; Gagne, S.;
702 Ickes, L.; Kurten, A.; Kupc, A.; Metzger, A.; Riccobono, F.; Rondo, L.; Schobesberger, S.;
703 Tsagkogeorgas, G.; Wimmer, D.; Amorim, A.; Bianchi, F.; Breitenlechner, M.; David, A.; Dommen, J.;
704 Downard, A.; Ehn, M.; Flagan, R. C.; Haider, S.; Hansel, A.; Hauser, D.; Jud, W.; Junninen, H.; Kreissl,
705 F.; Kvashin, A.; Laaksonen, A.; Lehtipalo, K.; Lima, J.; Lovejoy, E. R.; Makhmutov, V.; Mathot, S.;
706 Mikkila, J.; Minginette, P.; Mogo, S.; Nieminen, T.; Onnela, A.; Pereira, P.; Petaja, T.; Schnitzhofer, R.;
707 Seinfeld, J. H.; Sipila, M.; Stozhkov, Y.; Stratmann, F.; Tome, A.; Vanhanen, J.; Viisanen, Y.; Vrtala, A.;
708 Wagner, P. E.; Walther, H.; Weingartner, E.; Wex, H.; Winkler, P. M.; Carslaw, K. S.; Worsnop, D. R.;
709 Baltensperger, U.; Kulmala, M. Role of sulphuric acid, ammonia and galactic cosmic rays in atmospheric
710 aerosol nucleation. *Nature* **2011,** *476* (7361), 429-433.
711 56. Franchin, A.; Ehrhart, S.; Leppä, J.; Nieminen, T.; Gagné, S.; Schobesberger, S.; Wimmer, D.;
712 Duplissy, J.; Riccobono, F.; Dunne, E. M.; Rondo, L.; Downard, A.; Bianchi, F.; Kupc, A.; Tsagkogeorgas,
713 G.; Lehtipalo, K.; Manninen, H. E.; Almeida, J.; Amorim, A.; Wagner, P. E.; Hansel, A.; Kirkby, J.;
714 Kürten, A.; Donahue, N. M.; Makhmutov, V.; Mathot, S.; Metzger, A.; Petäjä, T.; Schnitzhofer, R.; Sipilä,
715 M.; Stozhkov, Y.; Tomé, A.; Kerminen, V. M.; Carslaw, K.; Curtius, J.; Baltensperger, U.; Kulmala, M.
716 Experimental investigation of ion–ion recombination under atmospheric conditions. *Atmos. Chem. Phys.*
717 **2015,** *15* (13), 7203-7216.
718 57. Yao, L.; Garmash, O.; Bianchi, F.; Zheng, J.; Yan, C.; Kontkanen, J.; Junninen, H.; Mazon, S. B.;
719 Ehn, M.; Paasonen, P.; Sipila, M.; Wang, M.; Wang, X.; Xiao, S.; Chen, H.; Lu, Y.; Zhang, B.; Wang, D.;

Fu, Q.; Geng, F.; Li, L.; Wang, H.; Qiao, L.; Yang, X.; Chen, J.; Kerminen, V. M.; Petaja, T.; Worsnop, D. R.; Kulmala, M.; Wang, L. Atmospheric new particle formation from sulfuric acid and amines in a Chinese megacity. *Science* **2018,** *361* (6399), 278-281.

58. Wang, M.; Chen, D.; Xiao, M.; Ye, Q.; Stolzenburg, D.; Hofbauer, V.; Ye, P.; Vogel, A. L.; Mauldin, R. L., 3rd; Amorim, A.; Baccarini, A.; Baumgartner, B.; Brilke, S.; Dada, L.; Dias, A.; Duplissy, J.; Finkenzeller, H.; Garmash, O.; He, X. C.; Hoyle, C. R.; Kim, C.; Kvashnin, A.; Lehtipalo, K.; Fischer, L.; Molteni, U.; Petaja, T.; Pospisilova, V.; Quelever, L. L. J.; Rissanen, M.; Simon, M.; Tauber, C.; Tome, A.; Wagner, A. C.; Weitz, L.; Volkamer, R.; Winkler, P. M.; Kirkby, J.; Worsnop, D. R.; Kulmala, M.; Baltensperger, U.; Dommen, J.; El-Haddad, I.; Donahue, N. M. Photo-oxidation of Aromatic Hydrocarbons Produces Low-Volatility Organic Compounds. *Environ. Sci. Technol.* **2020,** *54* (13), 7911-7921.

59. Kirkby, J.; Duplissy, J.; Sengupta, K.; Frege, C.; Gordon, H.; Williamson, C.; Heinritzi, M.; Simon, M.; Yan, C.; Almeida, J.; Tröstl, J.; Nieminen, T.; Ortega, I. K.; Wagner, R.; Adamov, A.; Amorim, A.; Bernhammer, A.-K.; Bianchi, F.; Breitenlechner, M.; Brilke, S.; Chen, X.; Craven, J.; Dias, A.; Ehrhart, S.; Flagan, R. C.; Franchin, A.; Fuchs, C.; Guida, R.; Hakala, J.; Hoyle, C. R.; Jokinen, T.; Junninen, H.; Kangasluoma, J.; Kim, J.; Krapf, M.; Kürten, A.; Laaksonen, A.; Lehtipalo, K.; Makhmutov, V.; Mathot, S.; Molteni, U.; Onnela, A.; Peräkylä, O.; Piel, F.; Petäjä, T.; Praplan, A. P.; Pringle, K.; Rap, A.; Richards, N. A. D.; Riipinen, I.; Rissanen, M. P.; Rondo, L.; Sarnela, N.; Schobesberger, S.; Scott, C. E.; Seinfeld, J. H.; Sipilä, M.; Steiner, G.; Stozhkov, Y.; Stratmann, F.; Tomé, A.; Virtanen, A.; Vogel, A. L.; Wagner, A. C.; Wagner, P. E.; Weingartner, E.; Wimmer, D.; Winkler, P. M.; Ye, P.; Zhang, X.; Hansel, A.; Dommen, J.; Donahue, N. M.; Worsnop, D. R.; Baltensperger, U.; Kulmala, M.; Carslaw, K. S.; Curtius, J. Ion-induced nucleation of pure biogenic particles. *Nature* **2016,** *533* (7604), 521-526.

60. Yan, C.; Yin, R.; Lu, Y.; Dada, L.; Yang, D.; Fu, Y.; Kontkanen, J.; Deng, C.; Garmash, O.; Ruan, J.; Baalbaki, R.; Schervish, M.; Cai, R.; Bloss, M.; Chan, T.; Chen, T.; Chen, Q.; Chen, X.; Chen, Y.; Chu, B.; Dällenbach, K.; Foreback, B.; He, X.; Heikkinen, L.; Jokinen, T.; Junninen, H.; Kangasluoma, J.; Kokkonen, T.; Kurppa, M.; Lehtipalo, K.; Li, H.; Li, H.; Li, X.; Liu, Y.; Ma, Q.; Paasonen, P.; Rantala, P.; Pileci, R. E.; Rusanen, A.; Sarnela, N.; Simonen, P.; Wang, S.; Wang, W.; Wang, Y.; Xue, M.; Yang, G.; Yao, L.; Zhou, Y.; Kujansuu, J.; Petäjä, T.; Nie, W.; Ma, Y.; Ge, M.; He, H.; Donahue, N. M.; Worsnop, D. R.; Kerminen, V. M.; Wang, L.; Liu, Y.; Zheng, J.; Kulmala, M.; Jiang, J.; Bianchi, F. The synergistic role of sulfuric acid, bases, and oxidized organics governing new-particle formation in Beijing. *Geophys. Res. Lett.* **2021,** *48* (7), e2020GL091944

61. Jen, C. N.; McMurry, P. H.; Hanson, D. R. Stabilization of sulfuric acid dimers by ammonia, methylamine, dimethylamine, and trimethylamine. *J. Geophys. Res.: Atmos.* **2014,** *119* (12), 7502-7514.

62. Kurten, T.; Loukonen, V.; Vehkamaki, H.; Kulmala, M. Amines are likely to enhance neutral and ion-induced sulfuric acid-water nucleation in the atmosphere more effectively than ammonia. *Atmos. Chem. Phys.* **2008,** *8* (14), 4095-4103.

63. Li, X.; Li, Y.; Lawler, M. J.; Hao, J.; Smith, J. N.; Jiang, J. Composition of Ultrafine Particles in Urban Beijing: Measurement Using a Thermal Desorption Chemical Ionization Mass Spectrometer. *Environ. Sci. Technol.* **2021,** *55* (5), 2859-2868.

64. Kurten, T.; Torpo, L.; Sundberg, M. R.; Kerminen, V. M.; Vehkamaki, H.; Kulmala, M. Estimating the NH3 : H2SO4 ratio of nucleating clusters in atmospheric conditions using quantum chemical methods. *Atmos. Chem. Phys.* **2007,** *7* (10), 2765-2773.

65. Cai, R.; Yan, C.; Yang, D.; Yin, R.; Lu, Y.; Deng, C.; Fu, Y.; Ruan, J.; Li, X.; Kontkanen, J.; Zhang, Q.; Kangasluoma, J.; Ma, Y.; Hao, J.; Worsnop, D. R.; Bianchi, F.; Paasonen, P.; Kerminen, V.-M.; Liu,

764 Y.; Wang, L.; Zheng, J.; Kulmala, M.; Jiang, J. Sulfuric acid–amine nucleation in urban Beijing. *Atmos.*
765 *Chem. Phys.* **2021,** *21* (4), 2457-2468.
766 66. Makkonen, U.; Virkkula, A.; Hellen, H.; Hemmila, M.; Sund, J.; Aijala, M.; Ehn, M.; Junninen, H.;
767 Keronen, P.; Petaja, T.; Worsnop, D. R.; Kulmala, M.; Hakola, H. Semi-continuous gas and inorganic
768 aerosol measurements at a boreal forest site: seasonal and diurnal cycles of NH_3, HONO and HNO_3.
769 *Boreal Environ. Res.* **2014,** *19*, 311-328.
770 67. Ge, X.; Wexler, A. S.; Clegg, S. L. Atmospheric amines – Part I. A review. *Atmos. Environ.* **2011,**
771 *45* (3), 524-546.
772

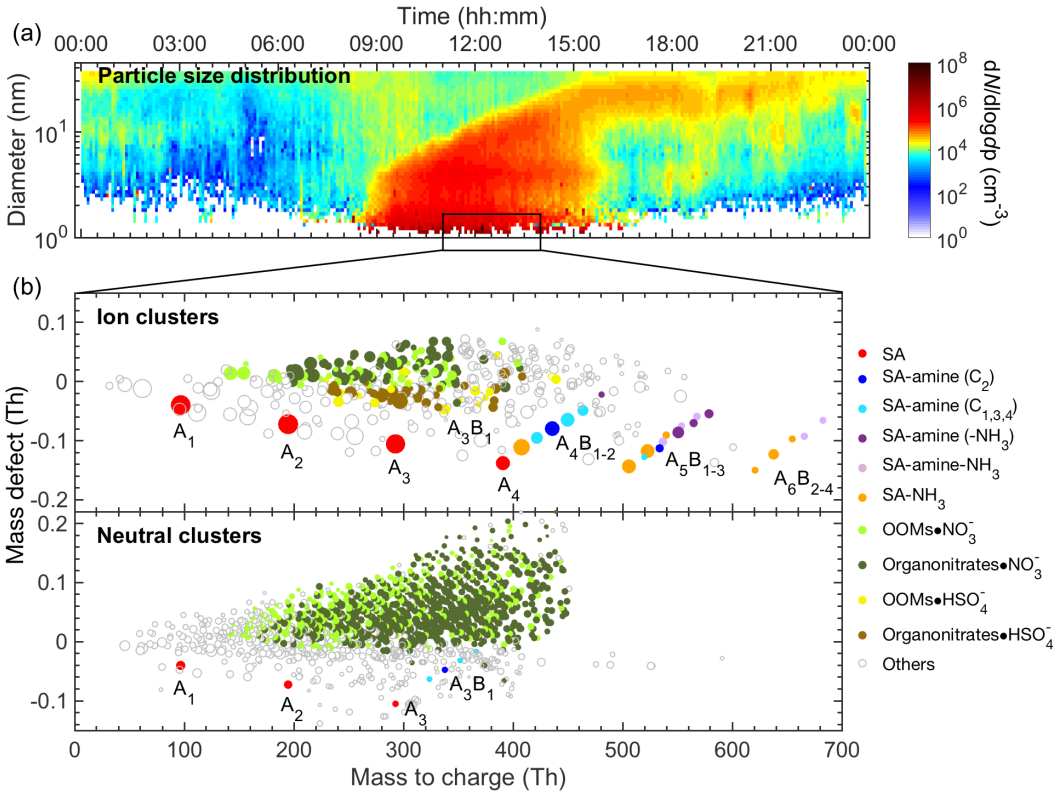

Figure 1. Particle size distributions (a), the composition of ion clusters and neutral clusters (b) in urban Beijing on Feb. 16th, 2018. The mass defect plots of ion clusters and neutral clusters were data averaged during the NPF period (i.e., 10:00 to 14:00). Mass defect is the difference between the exact mass and the nominal mass of the molecule or the cluster. The dot size is proportional to its signal intensity. The main species are acid-base clusters, organic clusters, and others. Acid-base clusters include sulfuric acid (SA), SA-amine (C_2), SA-amine ($C_{1,3,4}$), SA-amine(-NH_3), SA-amine-NH_3, and SA-ammonia (NH_3) clusters. A represent SA or bisulfate ion (HSO_4^-). B represent NH_3 or amines here. Organic clusters include oxidized organic molecules (OOMs) and organo-nitrate molecules charged by bisulfate ion or nitrate ion (NO_3^-).

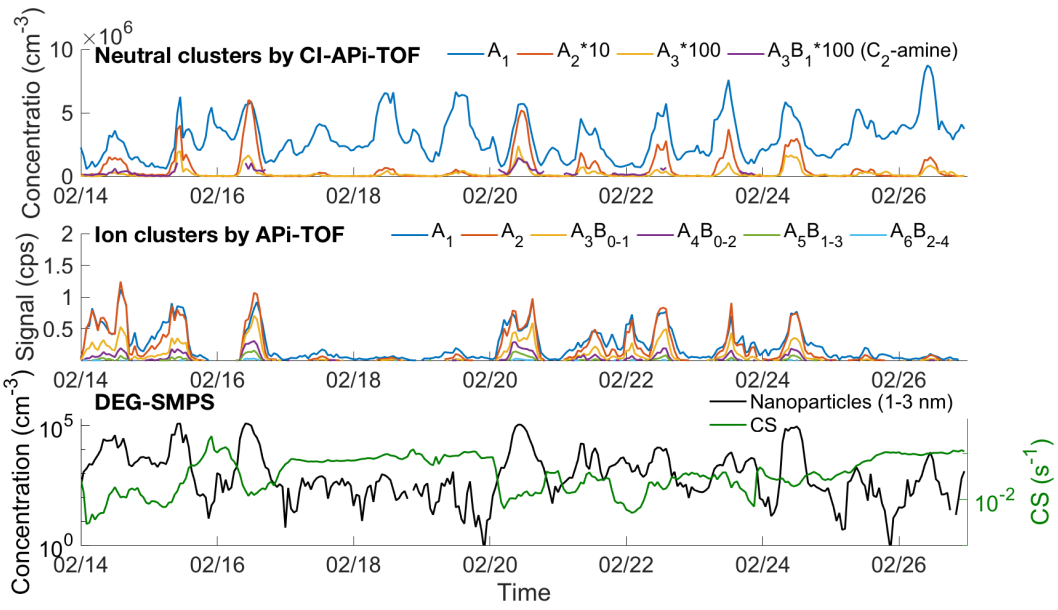

787

788 **Figure 2.** Time series of neutral and ion acid-base clusters in comparison to those of
789 sub-3 nm particles and condensation sink (CS). The data were obtained during Feb.
790 14^{th} to 27^{th}, 2018. Neutral acid-base clusters include monomer (A_1), dimer (A_2), and
791 trimer (A_3 and A_3B_1 containing C_2-amine). Ion acid-base clusters include monomer
792 (A_1), dimer (A_2), trimer (A_3B_{0-1}), tetramer (A_4B_{0-2}), pentamer (A_5B_{1-3}), and hexamer
793 (A_6B_{2-4}).

794

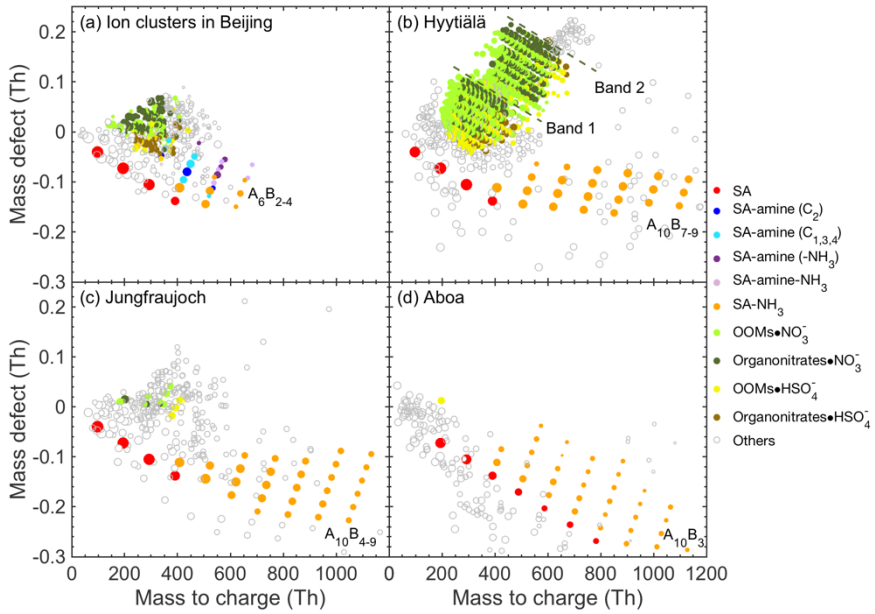

795

796 **Figure 3.** Ion acid-base clusters observed during NPF periods in (a) urban Beijing and
797 clean atmospheric environments such as (b) Hyytiälä[17], (c) Jungfraujoch[18], and (d)
798 Aboa[19].

799

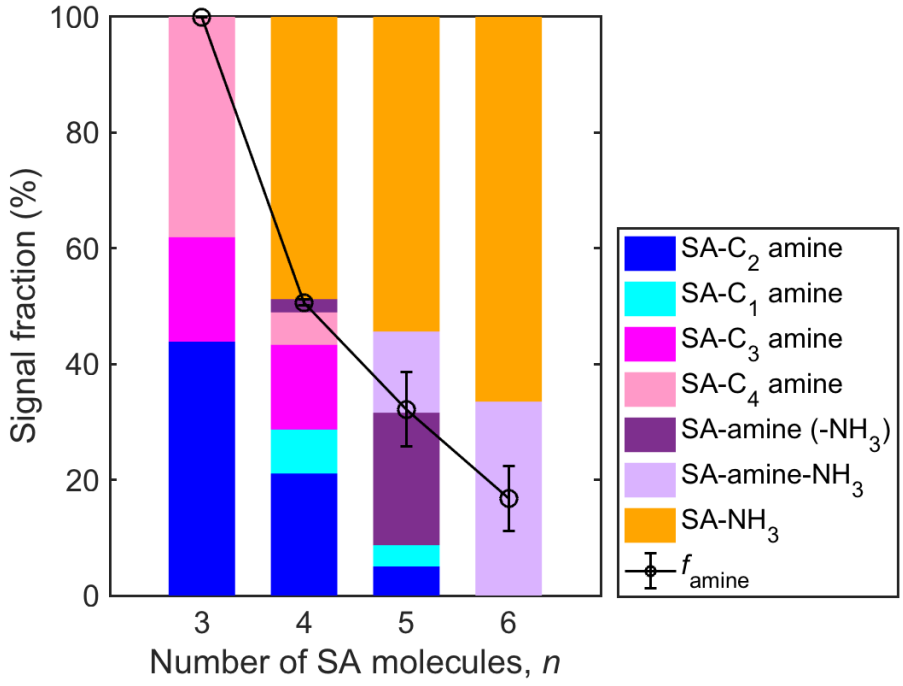

Figure 4. Compositions of ion acid-base clusters and their signal fractions as a function of the number of SA molecules. f_{amine} is the total fraction of amine-containing clusters, which includes the fraction of SA-amine clusters, part fraction of SA-amine-NH_3 clusters, and part fraction of SA-amine (-NH_3) clusters (Eq. S2). Error bars represent the minimum and the maximum of f_{amine} caused by the uncertainties of SA-amine (-NH_3) clusters. Data were obtained on Feb. 16th, 2018. SA clusters which do not contain base molecules are not included.

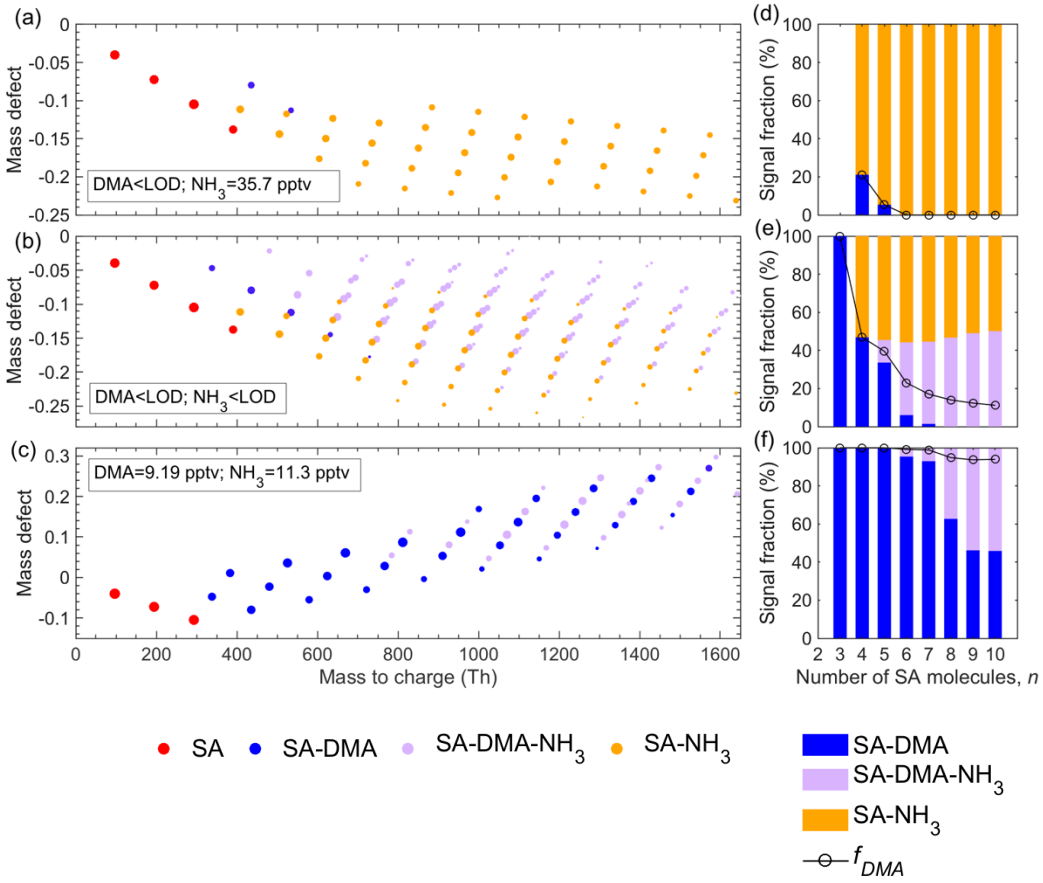

Figure 5. Ion acid-base clusters observed in three CLOUD experiments (a, b, c) and the fractions of SA-DMA clusters, SA-DMA-NH_3 clusters, and SA-NH_3 clusters as a function of the number of SA molecules (d, e, f) with different concentrations of DMA and NH_3. The concentrations for each experiment are presented in the plots. LOD is the limit of detection. In figure 5d, e, f, SA clusters which do not contain base molecules are not included. f_{DMA} is the total fraction of DMA-containing clusters, which includes the fraction of SA-DMA clusters and part fraction of SA-DMA-NH_3 clusters (Eq. S3), whose calculation is similar to that of f_{amine}. Detailed experiment conditions are given in Table S2. Note that the data of CLOUD experiments is adapted from Schobesberger et al.[3] and Bianchi et al [48].

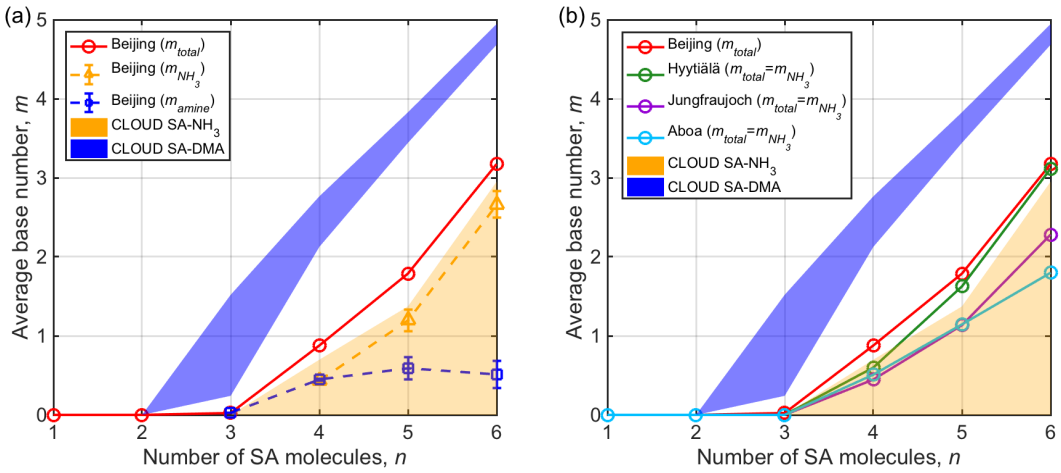

821

822 **Figure 6.** The average base number of ion acid-base clusters observed in Beijing in
823 comparison to those from CLOUD experiments (a) and clean atmospheric
824 enviornments such as Hyytiälä[17], Jungfraujoch[18], and Aboa[19] (b). Data of Beijing was
825 obtained on Feb. 16th, 2018 (the same to those used in Figure 1b). Error bars are the
826 maximum and the minimum of m_{NH3} and m_{amine}. Markers are their mean values. The
827 average base numbers in Hyytiälä, Jungfraujoch, and Aboa only include m_{NH3} actually,
828 as amine-containing clusters were not observed there. The ABN of ion acid-base
829 clusters in CLOUD experiments is calculated based on 14 sets of SA-DMA clustering
830 experiments and 23 sets of SA-NH_3 clustering experiments. Note that the data of
831 CLOUD experiments is adapted from Schobesberger et al [46].

Supplementary Information

Acid-base clusters during atmospheric new particle formation in urban Beijing

Rujing Yin[1], Chao Yan[2,3], Runlong Cai[3], Xiaoxiao Li[1], Jiewen Shen[4], Yiqun Lu[5], Siegfried Schobesberger[6], Yueyun Fu[1], Chenjuan Deng[1], Lin Wang[5], Yongchun Liu[2], Jun Zheng[7], Hongbin Xie[4], Federico Bianchi[2,3], Douglas R. Worsnop[3,8], Markku Kulmala[2,3], Jingkun Jiang[1]*

[1] State Key Joint Laboratory of Environment Simulation and Pollution Control, School of Environment, Tsinghua University, Beijing 100084, China.

[2] Aerosol and Haze Laboratory, Beijing Advanced Innovation Center for Soft Matter Science and Engineering, Beijing University of Chemical Technology, Beijing 100084, China.

[3] Institute for Atmospheric and Earth System Research / Physics, Faculty of Science, University of Helsinki, 00014 Helsinki, Finland.

[4] Key Laboratory of Industrial Ecology and Environmental Engineering (Ministry of Education), School of Environmental Science and Technology, Dalian University of Technology, Dalian 116024, China

[5] Shanghai Key Laboratory of Atmospheric Particle Pollution and Prevention (LAP3), Department of Environmental Science and Engineering, Fudan University, Shanghai 200433, China

[6] Department of Applied Physics, University of Eastern Finland, Kuopio, Finland

[7] Jiangsu Key Laboratory of Atmospheric Environment Monitoring and Pollution Control, Nanjing University of Information Science & Technology, Nanjing 210044, China

[8] Aerodyne Research Inc., Billerica, Massachusetts 01821, USA

11 pages

11 figures

2 tables

1. The calculation of the condensation sink (CS)

The condensation sink (CS) of sulfuric acid (SA) was calculated according to the method reported in Kulmala et al.[1] as below,

$$CS = 2\pi D \sum_{d_p} \beta_{m,d_p} d_p N_{d_p} \quad \text{(S1)}$$

where D is the diffusion coefficient of SA; β_m is the transitional correction factor; d_p is the particle geometric mean diameter; N_{dp} is the number concentration of particles of diameter d_p.

2.Calculation of the faction of amine-containing clusters (f_{amine})

The fraction of amine-containing clusters (f_{amine}) includes three parts, the total fraction of SA-amine clusters, part fraction of SA-amine-NH_3 clusters, and part fraction of SA-amine (-NH_3) clusters. The calculation is shown below:

$$f_{amine} = f_{SA-amine} + f_{SA-amine-NH_3} \times \frac{m_1}{m_1 + m_2} + f_{SA-amine\ (-NH_3)} \times \frac{m_1'}{m_1' + m_2'} \quad \text{(S2)}$$

where m_1 and m_2 are the number of amine and NH_3 molecules in SA-amine-NH_3 clusters, respectively; m_1' and m_2' are the number of amine and NH_3 molecules in SA-amine(-NH_3) clusters, respectively; $f_{\text{SA-amine}}$, $f_{\text{SA-amine-NH3}}$, and $f_{\text{SA-amine (-NH3)}}$ are the fractions of SA-amine clusters, SA-amine-NH_3 clusters, and SA-amine (-NH_3) clusters. Similarly, the calculation of the fraction of DMA-containing clusters (f_{DMA}) observed in CLOUD experiments is shown below:

$$f_{DMA} = f_{SA-DMA} + f_{SA-DMA-NH_3} \times \frac{m_1}{m_1 + m_2} \quad \text{(S3)}$$

where m_1 is the number of DMA molecules in SA-DMA-NH_3 clusters; m_2 is the number of NH_3 molecules in clusters; $f_{\text{SA-DMA}}$ and $f_{\text{SA-DMA-NH3}}$ are the fractions of SA-DMA clusters and SA-DMA-NH_3 clusters.

Table S1. Formulas of ion clusters observed in Beijing (and also shown in **错误!未找到引用源。**).

Number of SA, n[a]	Type[b]	Formula	m/z (Th)
1	A_1	HSO_4^-	96.9601
2	A_2	$(H_2SO_4)HSO_4^-$	194.9275
3	A_3	$(H_2SO_4)_2HSO_4^-$	292.8949
	A_3B_1	$(H_2SO_4)_2(C_2H_5NH_2)HSO_4^-$	337.9527
		$(H_2SO_4)_2(C_3H_9NH_2)HSO_4^-$	351.9684
		$(H_2SO_4)_2(C_4H_{11}NH_2)HSO_4^-$	365.9840
4	A_4	$(H_2SO_4)_3HSO_4^-$	390.8622
	A_4B_1	$(H_2SO_4)_3(NH_3)HSO_4^-$	407.8888
		$(H_2SO_4)_3(CH_3NH_2)HSO_4^-$	421.9044
		$(H_2SO_4)_3(C_2H_5NH_2)HSO_4^-$	435.9201
		$(H_2SO_4)_3(C_3H_7NH_2)HSO_4^-$	449.9357
		$(H_2SO_4)_3(C_4H_9NH_2)HSO_4^-$	463.9514
	A_4B_2	$(H_2SO_4)_3(C_2H_5NH_2)_2HSO_4^-$ or $(H_2SO_4)_3(C_4H_9NH_2)(NH_3)HSO_4^-$	480.9779
5	A_5B_1	$(H_2SO_4)_4(NH_3)HSO_4^-$	505.8562
		$(H_2SO_4)_4(CH_3NH_2)HSO_4^-$	519.8718
		$(H_2SO_4)_4(C_2H_5NH_2)HSO_4^-$	533.8875
	A_5B_2	$(H_2SO_4)_4(NH_3)_2HSO_4^-$	522.8827
		$(H_2SO_4)_4(CH_3NH_2)(NH_3)HSO_4^-$	536.8984
		$(H_2SO_4)_4(C_2H_5NH_2)(NH_3)HSO_4^-$ or $(H_2SO_4)_4(CH_3NH_2)_2HSO_4^-$	550.9140
		$(H_2SO_4)_4(C_3H_7NH_2)(NH_3)HSO_4^-$ or $(H_2SO_4)_4(C_2H_5NH_2)(CH_3NH_2)HSO_4^-$	564.9297
		$(H_2SO_4)_4(C_2H_5NH_2)_2HSO_4^-$ or $(H_2SO_4)_4(C_4H_9NH_2)(NH_3)HSO_4^-$	578.9453
	A_5B_3	$(H_2SO_4)_4(NH_3)_3HSO_4^-$	539.9093
		$(H_2SO_4)_4(CH_3NH_2)(NH_3)_2HSO_4^-$	553.9249
		$(H_2SO_4)_4(C_2H_5NH_2)(NH_3)_2HSO_4^-$ or $(H_2SO_4)_4(CH_3NH_2)_2(NH_3)HSO_4^-$	567.9406
6	A_6B_2	$(H_2SO_4)_5(NH_3)_2HSO_4^-$	620.8501
	A_6B_3	$(H_2SO_4)_5(NH_3)_3HSO_4^-$	637.8766
		$(H_2SO_4)_5(C_2H_5NH_2)(NH_3)_2HSO_4^-$ or $(H_2SO_4)_5(CH_3NH_2)_2(NH_3)HSO_4^-$	665.9079
	A_6B_4	$(H_2SO_4)_5(NH_3)_4HSO_4^-$	654.9032
		$(H_2SO_4)_5(C_2H_5NH_2)(NH_3)_3HSO_4^-$ or $(H_2SO_4)_5(CH_3NH_2)_2(NH_3)_2HSO_4^-$	682.9345

[a]The number of SA includes one bisulfate ion (HSO_4^-).

[b]A represents SA. B represents bases.

Table S2. Conditions of the CLOUD experiments displayed in Figure 5.

figure	run no.	run type	T (K)	H_2SO_4 (cm^{-3})	NH_3 (pptv)	DMA (pptv)

a, d	404.01	GCR	278.15	7.4e7	35.7	<LOD
b, e	1056.07	Beam	278.15	6.21e6	<LOD	<LOD
c, f	482.01	GCR	278.15	4.6e6	11.3	9.19

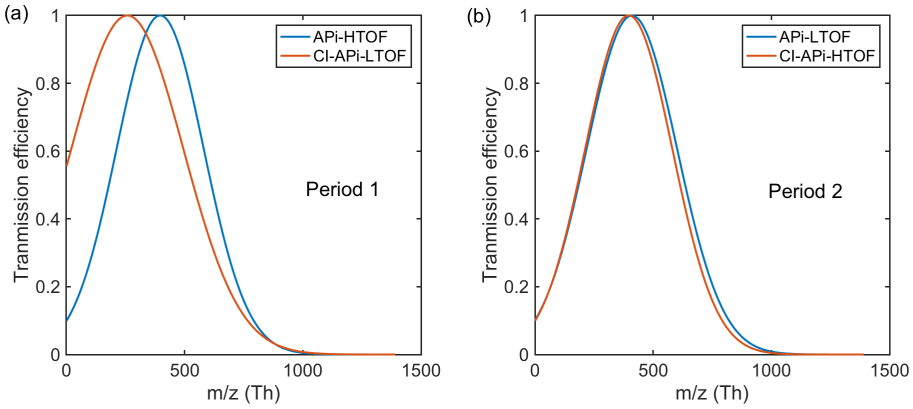

Figure S1. The relative transmission efficiencies of APi-TOF and CI-APi-TOF which were used to measure ion clusters and neutral clusters during period 1 (a) and period 2 (b), respectively.

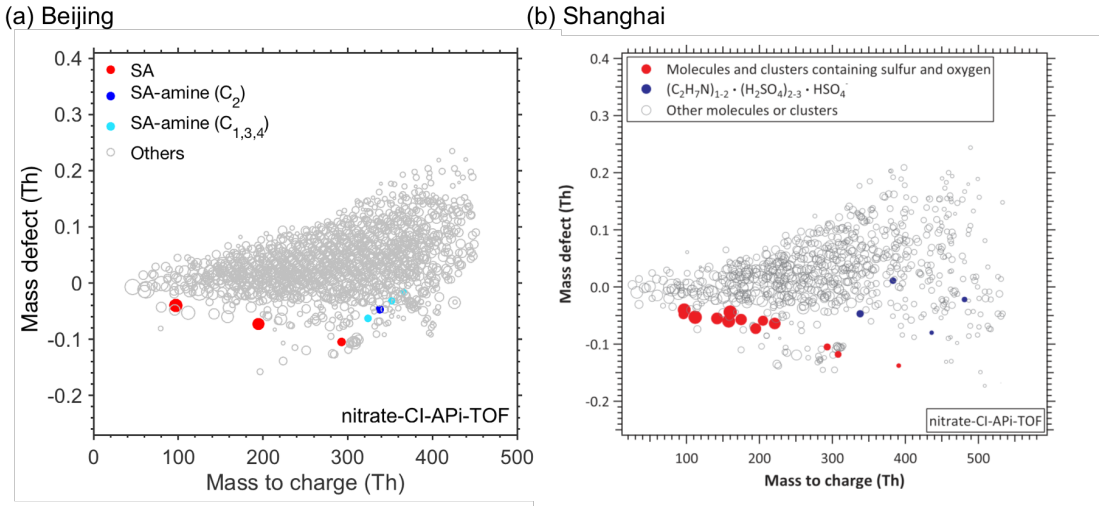

Figure S2. Neutral acid-base clusters observed during NPF periods in (a) Beijing and (b) Shanghai. SO_3^- and SO_5^- were marked red in Shanghai but not in Beijing. (The right panel is reprinted with the permission from ref. 2. Copyright 2018 Science.)[2]

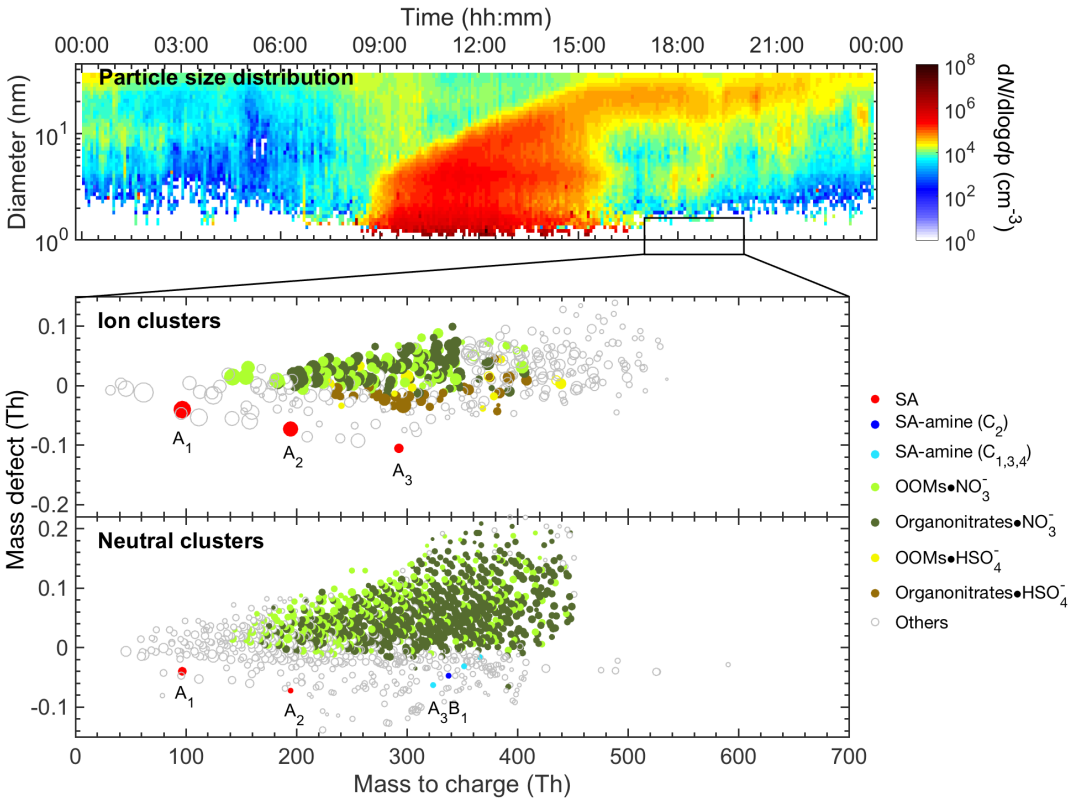

Figure S3. Particle size distributions (a), the composition of ion clusters and neutral clusters (b) after new particle formation (NPF) in urban Beijing on Feb 16th, 2018. The upper panel is the measured temporal evolution of particle size distributions. The lower panels are mass defect plots of ion clusters and neutral clusters detected by APi-TOF and CI-APi-TOF, respectively. Mass defect plots are averaged between 17:00 and 20:00. Mass defect is the difference between the exact mass and nominal mass of the molecule. The dot size is proportional to its signal intensity. The main species are acid-base clusters, organic clusters and other compounds. Acid-base clusters include sulfuric acid (SA), SA-amine (C_2), and SA-amine ($C_{1,3,4}$). Organic clusters include oxidized organic molecules (OOM) and organonitrates molecules charged by bisulfate (HSO_4^-) or nitrate (NO_3^-). Other compounds include some ion and organic acids. A represent SA or bisulfate. B represents amines here. Compared with results during the NPF, NH_3 or amines are not observed in ion clusters. Amines still turns up from SA trimer (A_3B_1) in neutral clusters. In the meantime, signals of A_1 and A_2 decreased and A_3 disappears.

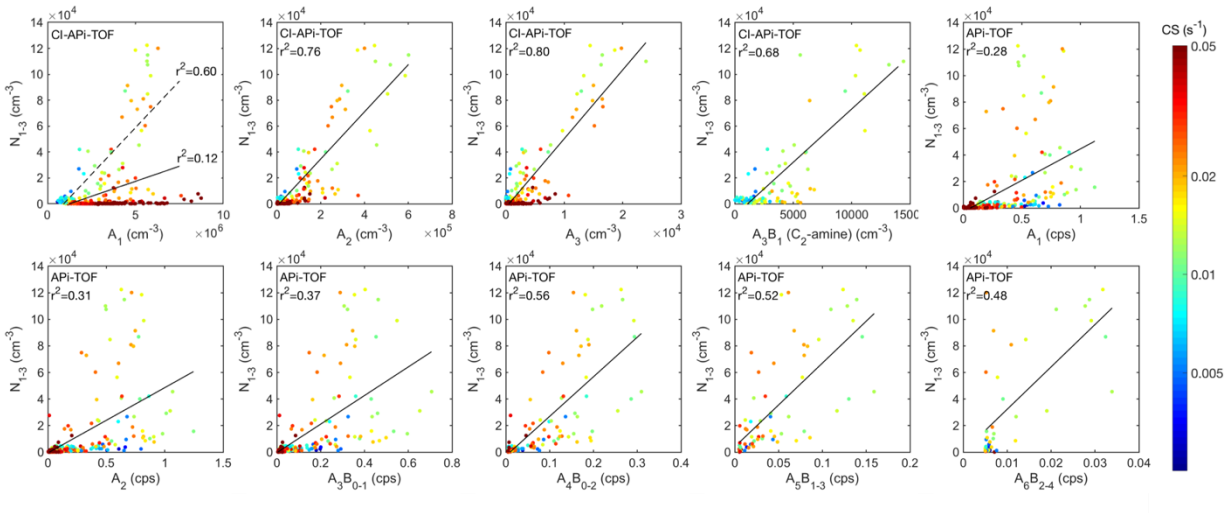

Figure S4. Scatter plot of neutral and ion acid-base clusters and sub-3 nm particles from Feb 14th to Feb 27th, 2018, as colored by condensation sink (CS). Black lines are their linear fitting and the correlation coefficients are marked on each plot. Sometimes gaseous SA (neutral A_1) was generated during nighttime in Beijing[3], while due to the high CS, NPF events did not happen. Dashed line is the linear fitting between neutral A_1 and sub-3 nm particles during NPF periods. The fitting of neutral A_3B_1 cluster with C_2-amines was influenced by the adjacent large peaks during non-NPF periods. Thus, only the concentration of neutral A_3B_1 cluster during NPF periods were used in our study. Neutral acid-base clusters were measured by CI-APi-TOF. Ion acid-base clusters were measured by APi-TOF.

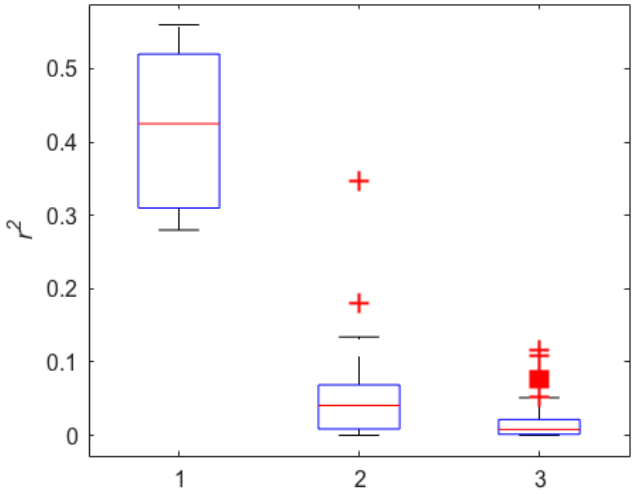

Figure S5. Box plot of the square of correlation coefficients (r^2) between signals of ion clusters and number concentration of sub-3 nm particles. 1 represents ion acid-base clusters. 2 represents ion OOM-HSO_4^- clusters. 3 represents ion OOM-NO_3^- clusters. Their median values are 0.423, 0.04, and 0.008, respectively.

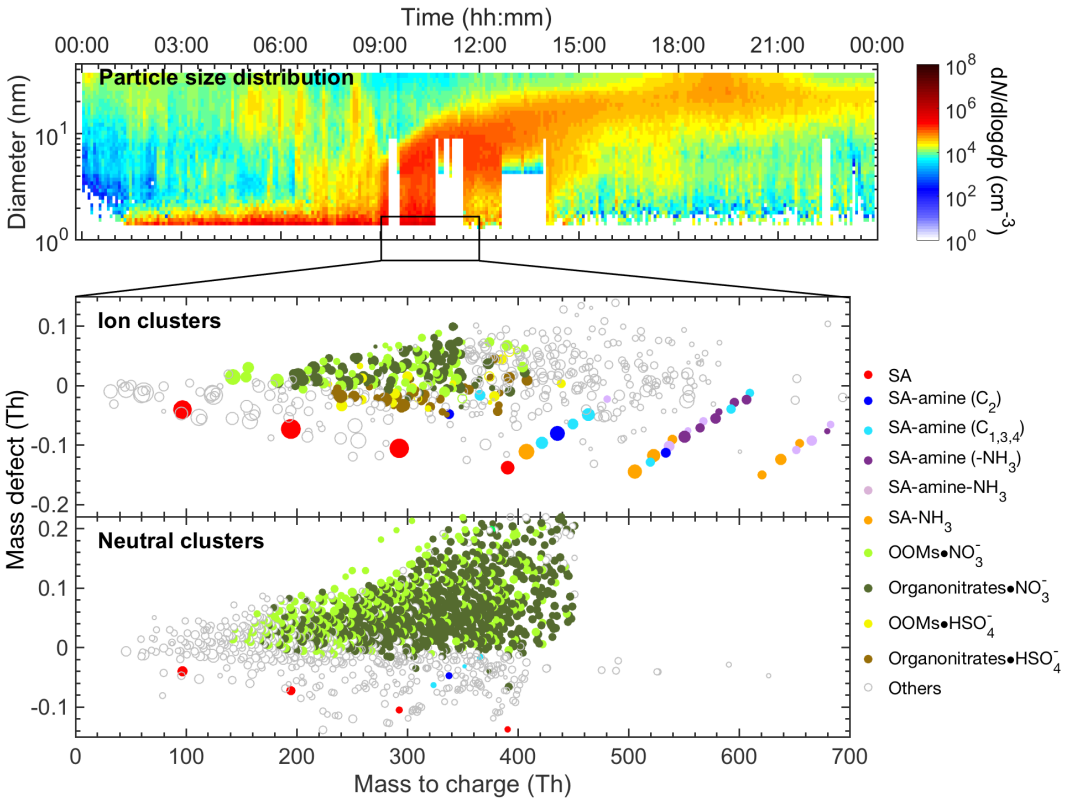

Figure S6. Particle size distribution (a), the composition of ion clusters and neutral clusters (b) after new particle formation in urban Beijing on Nov. 9th, 2018. The upper panel is the measured temporal evolution of particle size distributions. The lower panels are mass defect plots of ion clusters and neutral clusters detected by APi-TOF and CI-APi-TOF, respectively. Both neutral and ion clusters were averaged from 9:00 to 12:00. The dot size is proportional to its signal intensity.

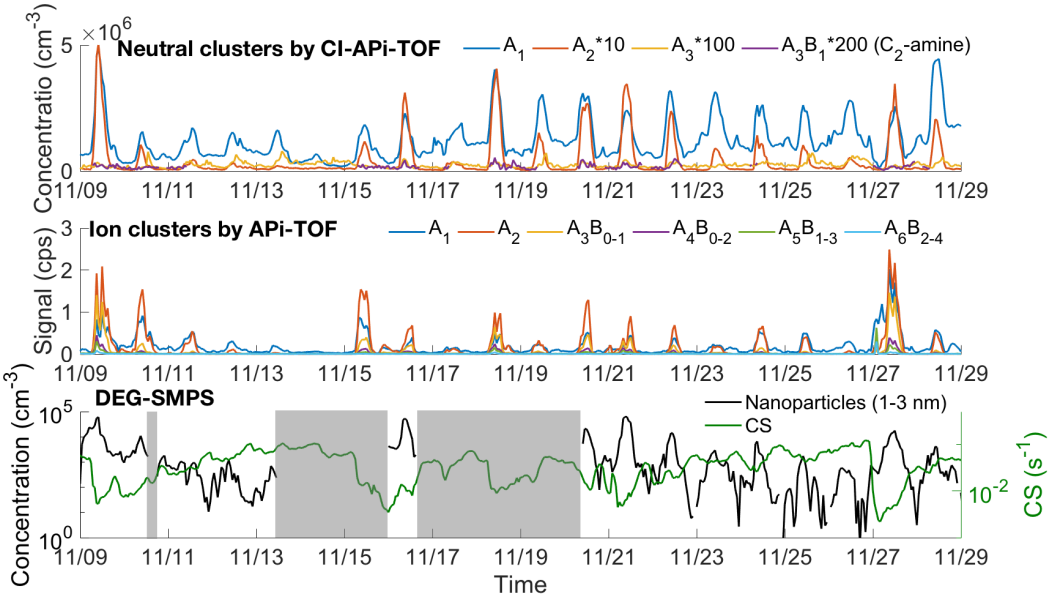

Figure S7. Time series of neutral and ion acid-base clusters in comparison to those of sub-3 nm particles and condensation sink (CS). The data were from Nov. 9th to 28th (period 2), 2018. The shadow part is the period when the concentration of sub-3 nm particles was absent.

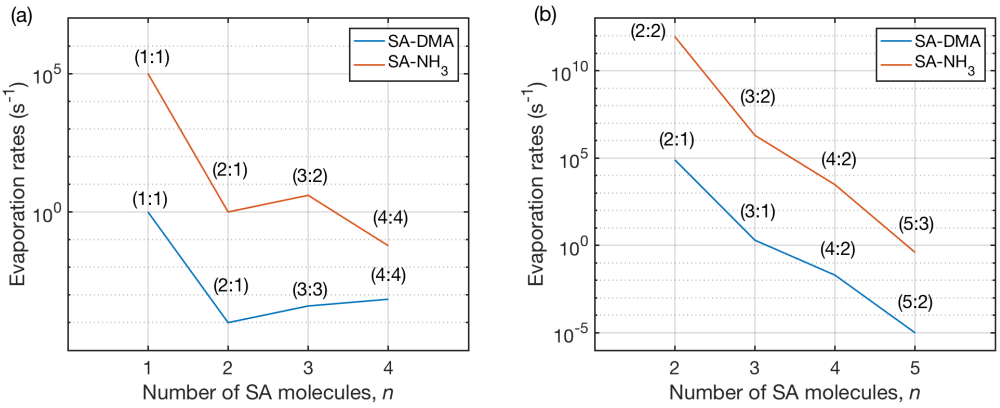

Figure S8. The evaporation rates of SA-DMA and SA-NH_3 clusters containing different number of SA molecules for neutral clusters (a) and negatively charged clusters (b). For negatively charged clusters, the bisulfate is counted as one SA. The data is adapted from Myllys et al [4]. Clusters with the lowest evaporation rates were plotted and their acid-base ratios were marked.

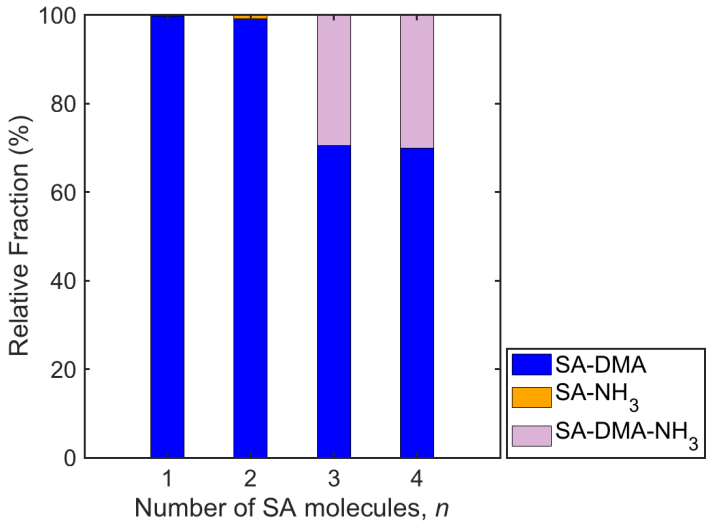

Figure S9. The ACDC simulated relative fractions of neutral acid-base clusters with different number of SA molecules from monomer to tetramer under the atmospheric conditions in urban Beijing (SA=2.6×10^6 cm^{-3}, DMA=1.8 pptv, NH_3=789pptv, CS=0.016 s^{-1}, T=278K). The ACDC simulation is based on the thermodynamic data of SA-DMA clusters, SA-NH_3 clusters, and SA-DMA-NH_3 clusters, which are from Li et al [5]. Monomers and dimers are mainly SA-DMA clusters. From trimers, SA-DMA-NH_3 clusters appear and they contribute to both trimers and tetramers.

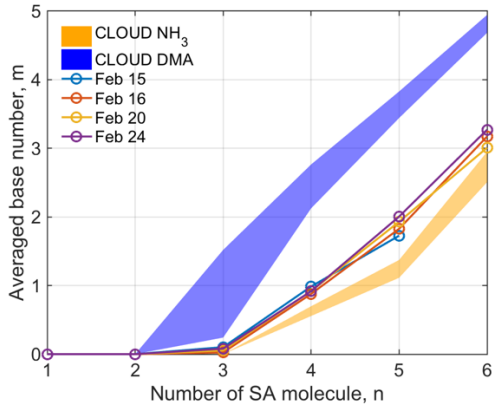

Figure S10. The m_{total} of acid-base clusters during NPF events in Beijing on different days.

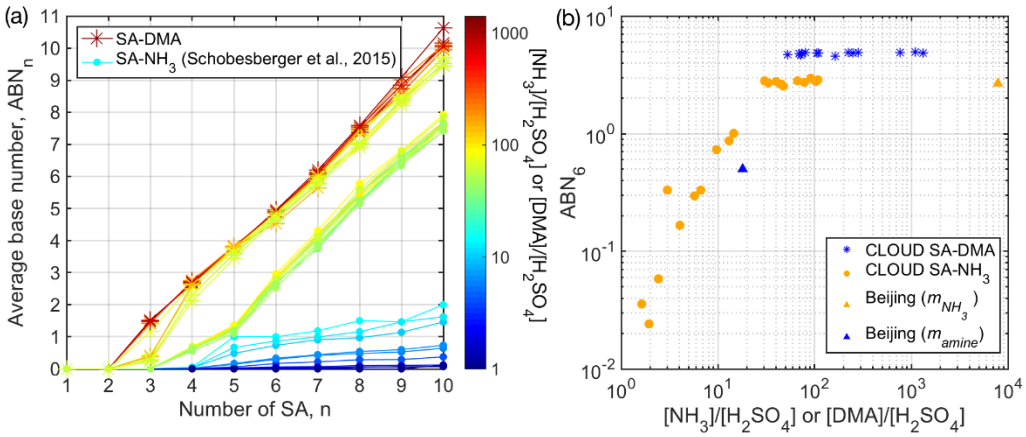

Figure S11. (a) Average base number (ABN) of SA-DMA ion clusters and SA-NH_3 ion clusters with different number of SA molecules in CLOUD chamber experiments, as colored by the ratio of gaseous bases to SA ([NH_3]/[H_2SO_4] or [DMA]/[H_2SO_4]); (b) ABN when the number of SA molecules is 6 (ABN_6) with different [NH_3]/[H_2SO_4] or [DMA]/[H_2SO_4] in CLOUD experiments and Beijing. These experiments were all performed under 278.15K. The concentrations of DMA and NH_3 in these experiments were between 5.84~141 pptv and 35~352 pptv, respectively. The concentrations of SA, DMA, and NH_3 used in Beijing is 1.8 pptv, 789 pptv and 2.6×10^6 cm^{-3}, respectively. Note that the data of CLOUD experiments is adapted from Schobesberger et al [6].

Reference

1. Kulmala, M.; Petaja, T.; Nieminen, T.; Sipila, M.; Manninen, H. E.; Lehtipalo, K.; Dal Maso, M.; Aalto, P. P.; Junninen, H.; Paasonen, P.; Riipinen, I.; Lehtinen, K. E.; Laaksonen, A.; Kerminen, V. M. Measurement of the nucleation of atmospheric aerosol particles. *Nat. Protoc.* **2012,** *7* (9), 1651-67.

2. Yao, L.; Garmash, O.; Bianchi, F.; Zheng, J.; Yan, C.; Kontkanen, J.; Junninen, H.; Mazon, S. B.; Ehn, M.; Paasonen, P.; Sipila, M.; Wang, M.; Wang, X.; Xiao, S.; Chen, H.; Lu, Y.; Zhang, B.; Wang, D.; Fu, Q.; Geng, F.; Li, L.; Wang, H.; Qiao, L.; Yang, X.; Chen, J.; Kerminen, V. M.; Petaja, T.; Worsnop, D. R.; Kulmala, M.; Wang, L. Atmospheric new particle formation from sulfuric acid and amines in a Chinese megacity. *Science* **2018,** *361* (6399), 278-281.

3. Guo, Y.; Yan, C.; Li, C.; Ma, W.; Feng, Z.; Zhou, Y.; Lin, Z.; Dada, L.; Stolzenburg, D.; Yin, R.; Kontkanen, J.; Daellenbach, K. R.; Kangasluoma, J.; Yao, L.; Chu, B.; Wang, Y.; Cai, R.; Bianchi, F.; Liu, Y.; Kulmala, M. Formation of nighttime sulfuric acid from the ozonolysis of alkenes in Beijing. *Atmos. Chem. Phys.* **2021,** *21* (7), 5499-5511.

4. Myllys, N.; Kubečka, J.; Besel, V.; Alfaouri, D.; Olenius, T.; Smith, J. N.; Passananti, M. Role of base strength, cluster structure and charge in sulfuric-acid-driven particle formation. *Atmos. Chem. Phys.* **2019,** *19* (15), 9753-9768.

5. Li, H.; Ning, A.; Zhong, J.; Zhang, H.; Liu, L.; Zhang, Y.; Zhang, X.; Zeng, X. C.; He, H. Influence of atmospheric conditions on sulfuric acid-dimethylamine-ammonia-based new particle formation. *Chemosphere* **2020,** *245*, 125554.

6. Schobesberger, S.; Franchin, A.; Bianchi, F.; Rondo, L.; Duplissy, J.; Kürten, A.; Ortega, I. K.; Metzger, A.; Schnitzhofer, R.; Almeida, J.; Amorim, A.; Dommen, J.; Dunne, E. M.; Ehn, M.; Gagné, S.; Ickes, L.; Junninen, H.; Hansel, A.; Kerminen, V. M.; Kirkby, J.; Kupc, A.; Laaksonen, A.; Lehtipalo, K.; Mathot, S.; Onnela, A.; Petäjä, T.; Riccobono, F.; Santos, F. D.; Sipilä, M.; Tomé, A.; Tsagkogeorgas, G.; Viisanen, Y.; Wagner, P. E.; Wimmer, D.; Curtius, J.; Donahue, N. M.; Baltensperger, U.; Kulmala, M.; Worsnop, D. R. On the composition of ammonia–sulfuric-acid ion clusters during aerosol particle formation. *Atmos. Chem. Phys.* **2015,** *15* (1), 55-78.